Eur. Phys. J. D (2023) 77:56
https://doi.org/10.1140/epjd/s10053-023-00630-8

THE EUROPEAN PHYSICAL JOURNAL D

Regular Article – Optical Phenomena and Photonics

Dusty plasma in active galactic nuclei

Bożena Czerny[1,a], Michal Zajaček[2,b], Mohammad-Hassan Naddaf[1,3,c], Marzena Sniegowska[1,3,4,d], Swayamtrupta Panda[5,e], Agata Różanska[3,f], Tek P. Adhikari[6,g], Ashwani Pandey[1,h], Vikram Kumar Jaiswal[1,i], Vladimír Karas[7,j], Abhijeet Borkar[7,k], Mary Loli Martínez-Aldama[8,l], and Raj Prince[1,m]

[1] Center for Theoretical Physics, Polish Academy of Sciences, Al. Lotników 32/46, 02-668 Warsaw, Poland
[2] Department of Theoretical Physics and Astrophysics, Faculty of Science, Masaryk University, Kotlářská 2, 611 37 Brno, Czech Republic
[3] Nicolaus Copernicus Astronomical Center, Polish Academy of Sciences, Bartycka 18, 00-716 Warsaw, Poland
[4] School of Physics and Astronomy, Tel Aviv University, 69978 Tel Aviv, Israel
[5] Laboratório Nacional de Astrofísica, MCTI, R. dos Estados Unidos 154, Itajubá 37504-364, Brazil
[6] Inter University Center for Astronomy and Astrophysics, Pune, Maharashtra 411007, India
[7] Astronomical Institute, Czech Academy of Sciences, Boční II 1401, 14100 Prague, Czech Republic
[8] Departamento de Astronomía, Universidad de Chile, Camino del Observatorio 1515, Santiago Casilla 36-D Correo Central, Chile

Received 20 November 2022 / Accepted 6 March 2023 / Published online 6 April 2023

Abstract. For many years we have known that dust in the form of a dusty-molecular torus is responsible for the obscuration in active galactic nuclei (AGN) at large viewing angles and, thus, for the widely used phenomenological classification of AGN. Recently, we gained new observational and theoretical insights into the geometry of the torus region and the role of dust in the dynamics of emerging outflows and failed winds. We will briefly touch on all these aspects and provide a more detailed update of our dust-based model (FRADO—Failed Radiatively Accelerated Dusty Outflow) capable of explaining the processes of formation of Balmer lines in AGN.

1 Introduction

Dust is present in all galaxies, both active and non-active, as it is one of the constituents of the interstellar medium (see for a review [56]). In galaxies, dust originates primarily from vigorous, stellar winds characteristic of evolved stars which enriched their chemical composition through nuclear burning. Supernovae explosions are notably efficient in ejecting a highly enriched material. Our Galaxy—Milky Way—also contains a considerable amount of dust [34,242].

We are located at a distance of about 8 kpc from the Galactic center, roughly in the Galactic plane, and so the nucleus is shielded from us by an enormous amount of extinction of the order of 25 mags in V-band (e.g., [156,157,194]). However, the Milky Way nucleus is not active at present stage, and its central black hole is currently dim and inactive. In active galactic nuclei (AGN), the dust located at inner ~ 10 pc plays a very specific role—which is directly associated with their enhanced accretion activity.

In this brief review, we attempt to summarize a broad range of topics related to the role of dust in AGN classification, the geometry of the dust distribution, the physical properties of the dust and its interaction with the gaseous medium, and the dynamics of the dusty medium. We summarize the unsolved problems and prospects in Sect. 11. Our review is far from complete, although we include several references to other works that are particularly relevant to the topic.

T.I.: Physics of Ionized Gases and Spectroscopy of Isolated Complex Systems: Fundamentals and Applications.

Guest editors: Bratislav Obradović, Jovan Cvetić, Dragana Ilić, Vladimir Srećkovićand Sylwia Ptasinska.

[a] e-mail: bcz@cft.edu.pl (corresponding author)
[b] e-mail: zajacek@mail.muni.cz
[c] e-mail: naddaf@cft.edu.pl
[d] e-mail: msniegowska@tauex.tau.ac.il
[e] e-mail: spanda@lna.br
[f] e-mail: agata@camk.edu.pl
[g] e-mail: tek@iucaa.in
[h] e-mail: ashwanitapan@gmail.com
[i] e-mail: vkj005@gmail.com
[j] e-mail: vladimir.karas@asu.cas.cz
[k] e-mail: abhijeet.borkar@asu.cas.cz
[l] e-mail: mmartinez@das.uchile.cl
[m] e-mail: raj@cft.edu.pl

2 Basic properties of AGN and the dusty torus in the standard unification scheme

Over the fifty years of the studies of quasars and even longer investigation of other types of active galaxies, such as Seyfert galaxies, radio galaxies and blazars, we have achieved a basic understanding of the structure of these objects (see monographs by [114,129], and reviews by [28,151] for a recent comprehensive overview of AGN properties). Every AGN consists of a supermassive black hole, and an inflowing material which determines the level of activity. The inflowing material usually possesses considerable angular momentum; close to the nucleus it must form a disk-like structure. In highly accreting sources, the plasma cools efficiently, and a standard accretion disk forms, roughly represented by the model of [199]. If the stream of material is less vigorous, the flow becomes hot and optically thin, at least in the innermost parts. Advection-Dominated Accretion Flow (ADAF) then represents a canonical example [144]. The actual geometry must be more complicated to explain the hard X-ray emission and the soft X-ray excess on top of the optical/UV Big Blue Bump coming from the cold disk [44] (for reviews and specific models, see e.g. [2,20,51]). The character of the flow in the outer parts is still under discussion and may have a character of the spherically symmetric flow [30] or disk-like shape, depending on the feeding mechanism, the role of stellar winds, etc. (see, e.g., for a review [215]).

Some AGN (about 10%) exhibit strong relativistic outflows in the form of jets, and these are classified traditionally as radio-loud objects or (more recently) as jetted objects (see, e.g., for a review [165]). Out of those objects, some have jets oriented close to the line of sight towards an observer, so the jet emission is boosted and frequently overshines the nuclear emission. In the later sections, we will concentrate on the radio-quiet (non-jetted) sources, where we have much better insight into processes going on near the black hole. In the case of radio-quiet sources, we follow processes which are sensitive to the flow description close to the event horizon (e.g., cold disk emission in UV, X-ray reflection spectrum in X-rays, including the iron Kα line, X-ray reverberation mapping, etc.), while in jetted sources the direct resolution gives insight only on the sub-parsec scale.

Radio-quiet sources (about 30% of them, [183,200,232]) frequently show broad and narrow emission lines. The line broadening must be caused by the dispersion in the velocity of the emitting material since the kinematic widths of narrow lines are of the order of a few hundred km s^{-1}, and the broad lines have line widths of the order of a few thousand km s^{-1}, while the expected thermal broadening is of the order of a few km s^{-1} [109]. The latter constraint comes from the fact that Balmer lines are intense, implying that the hydrogen is not fully ionized and the corresponding plasma temperature must be of the order of 10 000 K. Much higher temperature would lead to full ionization of hydrogen and Balmer lines would not be observed [42]. Therefore, the standard view is such that the emission comes mainly from clouds orbiting the central black hole at a distance of a fraction of a parsec (for broad lines) and above a parsec (for narrow lines). These regions are named the Broad Line Region (BLR) and the Narrow Line Region (NLR), respectively. The line emission is caused by the irradiation of plasma by the central region where most of the accretion energy is dissipated and re-emitted [162,247]. When broad lines are seen, narrow lines are also present, and this shows up as a complex line shape of a single line consisting of broad and narrow components.

The emission lines differ not only in emitted velocities but also in the mechanism of their formation. The Balmer lines are seen both as broad and narrow lines in a given source but some of the narrow lines coming from other elements are actually forbidden lines, such as the [OIII] line at λ5007 Å, which means that the density of the emitting material is much lower in the NLR (e.g., [15,21,101,138]). A broad (1000–3000 km s^{-1}) [OIII]λ5007 component has been also detected in some sources with high accretion rates. This component is mostly observed with a blue-shifted profile, which indicates that part of the [OIII]λ5007 is originates in an outflow [122,148,193,195,258]. The line width, in such cases, does not represent the Keplerian virialized motion but instead the accelerated outflow. Some sources also show a broad [OIII]λ5007 core at the rest frame or in redshifted wings [24,148].

A fraction of the sources shows only narrow lines. It was a puzzle for many years about why BLR is not visible in these objects. Most quasars show broad lines, but fainter Seyfert galaxies frequently did not show BLR, so Seyfert galaxies were further sub-classified as Seyfert 1 (with BLR) and Seyfert 2 (without BLR). Quasars were also divided into type 1 and type 2 by analogy, although type 2 is rare. The resolution came from polarimetric observations performed by [10] for the famous Seyfert galaxy NGC 1068 from the original list of active galaxies selected by Seyfert in his seminal paper [196]. When viewed under unpolarized light, the source did not show the BLR component, while, in the polarized light, the broad component of the Balmer Hβ line was clearly present. The interpretation was that a thick torus surrounds the nucleus, and the BLR is located closer than the torus, while the NLR is located further out. If the viewing angle is low (as measured with respect to the symmetry axis), the view of the nucleus is unobscured, and we can see both NLR and BLR line components, but if the viewing angle is high, the torus shields the BLR component. The BLR component is only revealed again in the polarized light since, in this case, we can detect only a small fraction of the total light that has been scattered by the low-density material filling the (almost empty) space around the torus. This torus is now known as a dusty/molecular torus, with an inner radius of about a parsec [112]. The torus itself is seen in the infrared part of the AGN spectrum. Since the dust sublimation temperature is of the order of 1500 K, the dust emission appears only at longer wavelengths. Dust cannot be much hotter—

it then evaporates and the material is changed into (rich in heavy elements) gaseous phase [14,106]. Further insight came from observing and modeling this source (e.g., [76,92,133]). The location of the dust is observationally very well constrained by the reverberation mapping (see for recent results [134]).

Thus, the dusty/molecular torus provided a key element in the unification picture of radio-quiet AGN. It implies that their structure is always the same; the apparent variety of types comes from different orientations. The truth is slightly more complex: the accretion rate onto the black hole is another key element. It is conveniently parameterized by the Eddington ratio, i.e., the ratio of the luminosity dissipated in the flow to the maximum luminosity of a spherical source in which the radiation pressure (calculated for fully ionized pure hydrogen) marginally balances the gravity of the central body. This ratio does not depend on the value of the black hole mass, which in AGN can range from a few hundred thousand solar masses to ten billion solar masses. Hence, it is a very convenient value to use, even if, with limitations; an AGN is neither spherically symmetric nor consists of pure hydrogen. In quasars, the Eddington rate is typically about 10 % (between 1 % and 100 %, see, e.g., [171], their Fig. 3, [127], their Fig. 3). In nearby AGN, it is frequently much lower. Thus, quasars seem to always have a torus, while for nearby sources, there may be a considerable fraction of true Seyfert 2 galaxies where there is no torus.

Spectra of faint sources are strongly dominated by starlight, so the corresponding polarization measurements are difficult, and broad lines are also difficult to distinguish against the strong starlight background. On the one hand, extremely inactive galaxies like the center of the Milky Way—Sgr A*—do not have a dusty torus (its Eddington ratio is about 10^{-9}; see, e.g., [68], [62]), but they also are most likely devoid of any BLR itself since the inner flow is optically thin (e.g., ADAF), and, the BLR clouds do not form [48,119,155]. On the other hand, careful observation of potentially true Seyfert 2 galaxy NGC 3147 with the Hubble Space Telescope revealed the existence of broad Hα line [26,27] although the Eddington ratio in this source is quite low, about 10^{-4}; in this case, the line was not shielded, instead, it was just difficult to detect. The sources are divided into HBLR (Hidden BLRL) sources, where the broad lines were finally detected, usually in the polarized light, and NHBLR (Non-Hidden) BLR, or bare Seyfert 2 galaxies. With advancing observational accuracy, some sources are reclassified as HBLR (e.g., [185]). The physical conditions (e.g., the limit for the Eddington ratio) needed for the absence of the BLR and the torus are not yet well specified. It remains to be seen if the true absence of the BLR is related to the absence of also the torus, which would then suggest a common origin of these two important elements of an AGN and (most probably) their relation to the cold standard accretion disk.

The Eddington rate also influences the shape of the broad-band spectrum that is related to the character of the inner flow close to the black hole. In higher Eddington sources (Eddington ratio above 1%), the inflow is in the form of a cold, optically thick, geometrically thin accretion disk described rather well by the standard model of [199] and its relativistic version [158]. As an alternative, the slim disk operates at very high Eddington rates [1]. The spectrum is dominated by the Big Blue Bump component (e.g., [45]). At lower Eddington rates, the inner flow is most likely optically thin, in the form of an advection-dominated accretion flow (ADAF; [96,144]). Various extensions of this scenario were proposed, particularly in the context of jetted sources, such as JED-SAD (jet emitting disk–standard accretion disk) models [70,177] or MAD (magnetically arrested disk) models [146,147]. The unification scheme actually requires three parameters: jet strength, orientation, and the Eddington rate. Apart from the issue about the torus, the unification scheme works surprisingly well over a wide range of black hole mass, and there is also a good analogy in spectral behavior between AGN and Galactic black holes of masses of the order of only 10 solar masses (e.g., [135,207]).

All three above-mentioned parameters strongly influence the broad band spectrum of an AGN. The nucleus itself is basically unresolved, however, by observing the spectrum and the variability of the source the AGN structure can be constrained. Only two nearby objects have been resolved so far: the radio galaxy M87 and the center of the Milky Way—Sgr A*—were resolved by the Event Horizon Telescope to such an extent that the shadow, or silhouette, of the central black hole, is revealed and the innermost pattern of the hot flow in semi-circular motion [67,68] is seen. These interferometrical observations were performed in the millimeter regime, optimized for the resolution and the extinction. The detected signal was the synchrotron emission from hot, low-density plasma. We note that both objects are examples of sources at very low Eddington rates, so no cold disk was observed.

3 On the coexistence of the hot and cold dust-less plasma

The spectral complexity of AGN—broad band continuum and various types of emission lines—implies that the plasma in AGN has a broad parameter range for the density and ionization state. In addition, AGN shows a range of absorption lines that arise from the plasma located along the line of sight towards the black hole, where most of the optical/UV/X-ray emission is produced. These lines are phenomenologically characterized by their width, strength, and ionization of the corresponding ions. We thus have narrow absorption lines (NAL; e.g., [64,236]), broad absorption lines (BAL; e.g., [38,244]), warm absorbers (WA; e.g., [5,90,143]), and the ultra-fast outflows (UFO; e.g., [223]). The distance of the material forming those lines is difficult to estimate because we cannot identify the line widths or shifts with Keplerian motion, the way we do it for the BLR.

It may be that some of these absorption lines are actually due to BLR or NLR, seen in absorption instead of emission. Absorption lines imply a clumpy structure of the absorbing medium since numerous kinematic components are observed, particularly in UV, with different velocity shifts to the rest frame of an AGN.

That scenario might pose a problem with cloud stability since a dense, non-self-gravitating cloud in space would expand on the dynamical timescale and will eventually get dispersed. However, if cooler, denser clouds are indeed embedded in much hotter, low-density, fully ionized plasma, they can be stabilized. This scenario is well justified theoretically. As pointed out by [116] in the context of AGN, irradiated plasma is subject to thermal instability, and within a certain range of the gas pressure, two solutions for the gas temperature can co-exist—a low-density hot plasma, at the temperature of the order of 10^7 K, which heats and cools by the Compton process, and colder, denser plasma at the temperature of the order of 10^4 K, which mostly heats and cools by atomic processes. In general, all radiative processes are important in partially ionized plasma, and they include Comptonization (heating and cooling), free-free transitions, bound-free as well as bound-bound transitions. Thus, plasma at two extremely different temperatures can coexist. The equilibrium curves are conveniently shown using the ionization parameter Ξ introduced by [116],

$$\Xi = \frac{F_{\rm ion}}{nkTc}, \tag{1}$$

where $F_{\rm ion}$ is the ionizing flux between 1 and 10^3 Rydberg, n is the local number density, T is the medium temperature, k is the Boltzmann constant, and c is the speed of light. This parameter is dimensionless, and it measures the ratio of the radiation pressure to gas pressure.

The colder clouds can be in equilibrium when they are located on the equilibrium curve at an identical value of Ξ on the lower and upper branches. The intermediate branch is unstable, and under small perturbations, the plasma rapidly evolves on the thermal timescale towards one of the stable branches.

The coexistence of the two plasma states with a sharp discontinuity is more complex. Clouds out of equilibrium can reach equilibrium, but they can also slowly grow through condensation or disappear by evaporation. Computations of clouds out of equilibrium require the inclusion of an additional process: electron conduction, which is important at the sharp border between the two phases, where the temperature gradient is significantly large. This was recognized by [71] and subsequently studied in several papers in the context of AGN, both for the transition between the colder disk and the hotter plasma at the disk corona and for the warm absorber (WA) and BLR clouds (e.g., [19,37,189]). These computations require proper treatment of the radiative processes. Complex radiative transfer codes are used, such as CLOUDY [69], which allow us to calculate the ionization state of the material, and its temperature and perform the radiative transfer. The conduction term is frequently neglected if only the stationary solution is of interest, but then there are problems with the uniqueness of the solution under constant pressure.

Numerous papers employ the equilibrium curve for the discussion of the properties of the multi-phase medium in the context of AGN. For example, [179] used the equilibrium curves to address the cloud formation in the colliding AGN-supernovae winds. Several authors (e.g., [3,5,88,115]) considered the pressure balance in different phases of the WA medium. The issue is further complicated if we consider outflowing medium [49,240], or even supersonic outflow velocities [241].

The scenario of the coexistence of the colder clouds and the intercloud medium was also formulated as the radiation pressure confinement (RPC) of the clouds (see and the references therein [17,214]). In any case, the rough pressure balance and approximate thermal equilibrium allow for cloud formation and relatively long cloud existence. There are, however, mechanisms destroying such clouds (see discussion in [137]), e.g., in cloud collisions, the action of tidal forces, Kelvin-Helmholtz instability, etc. The clumpy medium is always dynamic. The same is true for the interstellar medium, although timescales in AGN are much shorter due to the smaller sizes of the clouds and much higher local densities.

4 Coexistence of the hot and cold dusty plasma

While the conditions of coexistence of the hot $T \sim 10^7$ K and warm $\sim 10^4$ K plasma was frequently discussed in the context of AGN (see Sect. 3), the coexistence of the third phase, cold dust $T < 1500$ K with the other two phases is less well studied from the physical point of view. On the other hand, we know that the dust is present within the central 1 pc as the dusty/molecular torus (see Sect. 2). In the advanced torus models, the clumpiness of the medium is included (e.g., [149,150,203,209,210]) since otherwise the more distant parts of the torus are not adequately illuminated and the model does not reproduce the observed silicate features in absorption or emission. The intercloud medium is usually neglected, like in [149,150], [210], and [203], who include the inter-cloud dust but not the inter-cloud gas phase.

The first extremely influential paper which addressed the issue of the dusty plasma interaction with the incident radiation was published by [152]. Their study of the dusty plasma and its efficiency in the production of emission lines showed that the presence of dust strongly suppressed the line emissivity, and, thus, they showed that the gap between the BLR and NLR (see Sect. 2) is caused by the presence of the dust. This way one of the key puzzles in AGN was explained.

However, later, a new sub-type of AGN was introduced
—Narrow Line Seyfert 1 galaxies [163]. These sources are different from type 2 sources, they exhibit broad lines, but much narrower than in typical Seyfert galaxies, and their forbidden lines are weak, unlike in Seyfert 2 objects. A formal definition included the maximum width of the lines of 2000 km s^{-1}. Later, for quasars which typically have much higher mass, a similar new class was introduced, i.e., type A (with the limit of the line width of 4000 km s^{-1}), while typical quasars were classified as type B, with broader lines [217]. Subsequent studies showed that these sources accrete close to the Eddington limit and, they form a high accretion rate tail of all AGN [168,172]. In addition, these objects do not show two-component line profiles, and their line profiles can be fitted by a single Lorentzian shape (e.g., [110,217,256]). The explanation of this lack of the BLR–NLR gap in these sources was solved by [4] where the authors showed that if the medium density is high enough, then the dust does not compete efficiently for photons with the partially ionized plasma. The gap postulated by [152] does not form, and indeed objects accreting at a high Eddington rate have a higher local density in the BLR than less vigorously accreting sources [171].

The coexistence of the three phases in AGN was finally studied in detail by [31] using the CLOUDY code in the context of high-resolution observational data for Centaurus A from ALMA and Chandra. We constructed the equilibrium curves for dusty plasma irradiated by hard X-rays from the central region (see Fig. 1). Here, the temperature T is the plasma temperature. We notice that without dust, the temperature saturates just below 10^4 K, even for a low value of the ionization parameter Ξ. Only at the distance of $\sim$ 200 pc does the temperature drop below 10^3 K. At the highest values of Ξ, the plasma temperature saturates at Inverse Compton temperature, about 10^8 K for the adopted shape of the radiation spectrum. We see the unstable branch corresponding to the negative slope of the stability curve. This agrees with the possibility of the coexistence of warm and hot plasma. However, in the presence of the dust, the temperature drops to much lower values for high Ξ, forming, at this location, an additional branch of solutions with an instability present at $\Xi \sim 10^{-5}$. There we can have a coexistence of cold and warm plasma.

For high Ξ, the temperature of the dusty plasma is much lower due to the interaction with dust grains. At $\Xi \sim 100$, there is a narrow range of the coexistence of the warm and hot plasma. Note that the temperature of the dusty plasma can be as high as 10^7 K. The dust can still exist, and its temperature is lower than the sublimation temperature, as reported by the CLOUDY code, but the dust temperature is not plotted. Thus, the dusty medium at high Ξ is a two-temperature medium, with individual cold dust grains embedded in the hot plasma. This is possible due to the low density of the hot plasma.

The computations thus show two ranges of Ξ at which a clumpy medium can form, but all three phases cannot coexist. A cold, dusty cloud cannot be in pressure equilibrium with the hot plasma, at least in the presented computations that consider an optically thin medium. In the optically thick medium, such coexistence is, perhaps, possible but the code CLOUDY cannot be used to describe such a scenario. Computations performed by [31] also did not address the processes taking place closer to the black hole within the BLR medium.

In the computations we used the currently most representative broad band spectrum of Cen A to describe the incident radiation, as given in Fig. 4 of [31]. The result may depend on this assumption, so it is not necessarily good for all sources. We also neglected the dust destruction mechanisms. As estimated by [58], the thermal sputtering rate for graphite, silicate, or iron grains at rest in hot gas with $10^6 < T < 10^9$ K is of the order of

$$\tau_{\rm sp} = 2 \times 10^4 \left(\frac{\rm cm^{-3}}{n_H}\right) \left(\frac{a}{0.01 \mu m}\right) \ [\rm yr], \qquad (2)$$

so for the two-temperature dusty region in our computations, the densities are smaller than $\sim$ 1 cm^{-3}, and the timescale is of the order of years. However, if strong shocks are present, the dust destruction is more efficient [57].

During the photoionization process by intense X-rays near an active nucleus, the dust grains develop an electric charge that is attached to their surface, and thus, a complex dusty plasma is formed [59,99,233,243]. Collective effects between the dust and gaseous components are essential in this environment, and the dust grain properties are different from those observed in the local interstellar medium. It has been argued that in AGN the dust grains suffer destruction by charging (e.g., and further references cited therein [222]), and the dust can be thus depleted. Also, the equilibrium structure of dusty tori may be significantly altered by the interplay of gravitational and electromagnetic forces that combine near accreting black holes in contrast with the classical test-fluid solutions. In our works [113,226] we have investigated the emerging structure of the charged tori, which may be quite different from the globally neutral ones. Especially their vertical extent and stability are affected [227].

5 Coexistence of hot and warm dusty plasma in the Galactic center

The Galactic center serves as the nearest to us prototype of a low-luminosity galactic nucleus. The bolometric luminosity of the compact variable source Sgr A*, which is associated with the supermassive black hole of $M_\bullet \sim 4 \times 10^6 M_\odot$ [50,62,79], is $L_{\rm SgrA*} \lesssim 10^{37} \sim 2600 L_\odot \, {\rm erg \, s^{-1}}$ [145]. The comparison with the Eddington luminosity $L_{\rm Edd} = 5.03 \times 10^{44} (M_\bullet / 4 \times 10^6 M_\odot) \, {\rm erg \, s^{-1}}$ for a given mass yields the Eddington ratio of $\lambda_{\rm Edd} = L_{\rm SgrA*}/L_{\rm Edd} \lesssim 2 \times 10^{-8}$. However, the source is variable

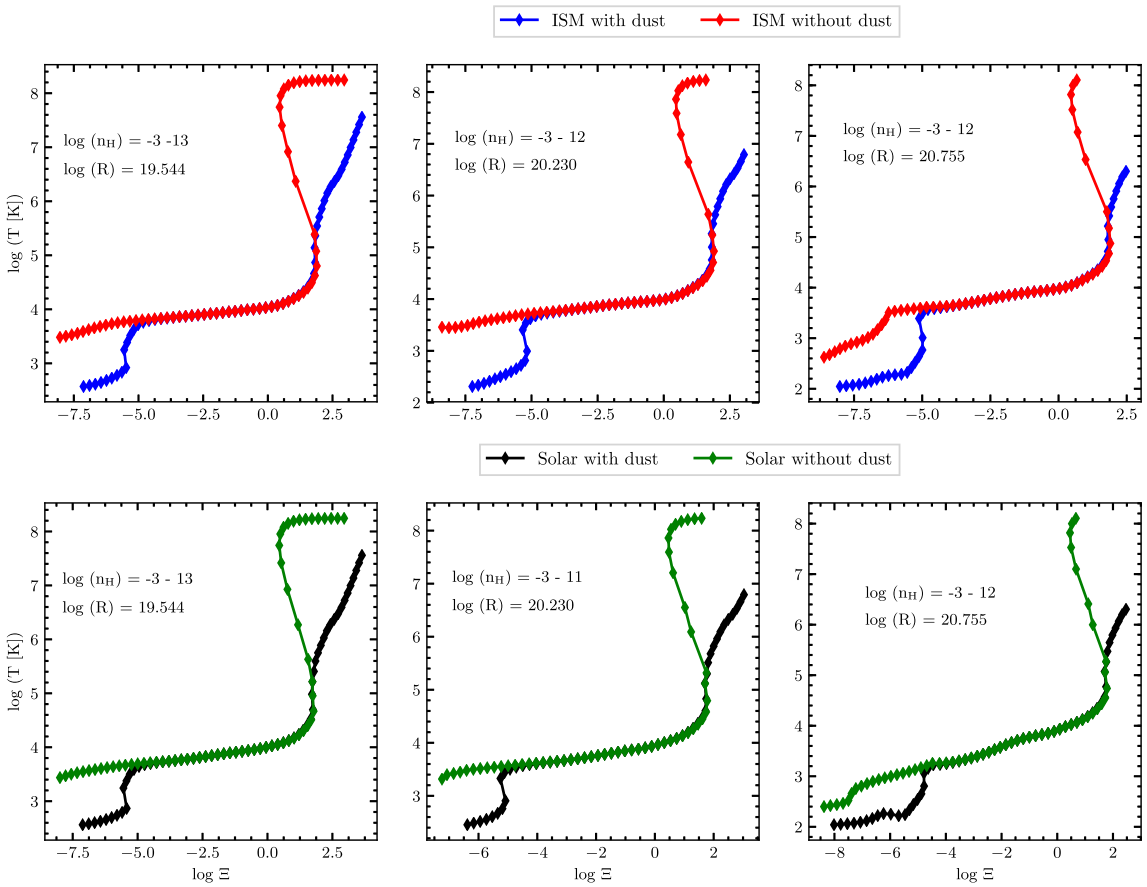

Fig. 1 Stability curves for the circumnuclear medium for two different, heavy element abundances: upper panels show ISM abundances, while bottom panels show solar abundances, with increasing radii from left to right: 11.5, 55, and 180 pc. Each panel contains calculations with and without dust. Each point in the curve represents the model computed for one starting value of density. The range density range is given in each panel. The SED luminosity is always kept at $L_{bol} = 10^{43}$ erg s^{-1} (from [31])

with order-of-magnitude near-infrared and X-ray flares taking place a few times per day (see, e.g., andreferencestherein [249]), which appears to be related to the hot plasma components with the size of ~ 4 gravitational radii and the temperature of $\sim 10^{10}$ K, the electron density of $4 \times 10^7\,\mathrm{cm}^{-3}$, and the magnetic field of ~ 10 G orbiting close to the innermost stable circular orbit in the form of "hot spots" [84,245]. There are several signatures that the accretion rate was significantly larger on the timescale of several hundred to million years, which has been revealed by the reprocessing of the central X-ray emission by the surrounding molecular clouds [218,219] and by the large-scale γ-ray emitting *Fermi* bubbles and the X-ray emitting *eRosita* bubbles [180,216].

Because of the current low Eddington ratio, the accretion flow surrounding Sgr A* is hot and diluted with low radiative efficiency. It can be modeled in the framework of advection-dominated accretion flows (or ADAFs) with a large scale-height-to-radius ratio approaching unity. On the larger scale, the flow is Bondi-like with power-law temperature and density profiles of the hot plasma with the asymptotic values of $n \sim 26\,\mathrm{cm}^{-3}$ and $T \sim 1.5 \times 10^7$ K at the Bondi radius [13], which can be estimated as follows,

$$R_\mathrm{B} = \frac{2GM_\bullet}{c_\mathrm{s}^2} \simeq \frac{2GM_\bullet \mu m_\mathrm{H}}{kT} \sim 0.14 \left(\frac{M_\bullet}{4 \times 10^6\,M_\odot}\right)\left(\frac{T}{1.5 \times 10^7\,\mathrm{K}}\right)^{-1} \mathrm{pc}\,, \tag{3}$$

where c_s is the asymptotic sound speed in the plasma. The Bondi radius expressed by Eq. (3) corresponds to $R_\mathrm{B} \sim 7.3 \times 10^5$ gravitational radii. However, the X-ray surface brightness is better described by a flatter density profile than for the standard Bondi inflow, i.e., $n \propto r^{-3/2+s}$, where $s \sim 1$, which implies the presence of an outflow [239].

The ADAF is located inside the Bondi radius, which is well within the ionized *central cavity* with the radius of $\sim$ 1–1.5 parsecs filled mostly with hot X-ray emitting optically thin plasma. In this region, which is also referred to as Sgr A West, there are distinct thermal streamers known as the Minispiral, whose kine-

matics is consistent with three bundles of Keplerian orbits around Sgr A* corresponding to the Northern Arm, Eastern Arm, and the Western Arc [261,262]. The Minispiral is well detected in the mid-infrared domain [25], which reveals the dust emission, and also in the sub-millimeter, millimeter, and the radio domains [136,228]. The electron density of the Minispiral is in the range of 3–21 $\times 10^4\,\mathrm{cm}^{-3}$ and the electron temperature is 5 000–13 000 K [117,262]. The highest densities of $21 \times 10^4\,\mathrm{cm}^{-3}$ are coincident with the IRS 13 region, while the highest temperature of 1.3×10^4 K is in the Bar region where the Northern and the Eastern Arms appear to collide at $\sim$ 0.1–0.2 pc south of and behind Sgr A* [262]. The dust density traces the ionized gas density along the three arms, which leads to the emission enhancement in the mid-infrared domain in the clumps along the Minispiral as well as at the places where supersonic stars flow through the ambient plasma and create denser bow shocks [186,192,220,221]. This shows that dust is generally coupled to gas via gas drag like in the standard interstellar medium, and the dust-to-gas mass ratio of 1:100 [29] is usually adopted for basic estimates.

Towards the Galactic center, the near-infrared emission (2.2 μm) is moderately polarized with the mean degree of $\sim$ 4% and the position angle of $\sim$ 30° along the Galactic plane. This foreground polarization is apparently due to anisotropic scattering of infrared radiation on elongated dust grains that are aligned along the Galactic spiral arms between the Earth and the Galactic center [60,164]. The presence of dust grains that are dynamically coupled to the sheared gas along the orbiting Minispiral arms can also be revealed via the polarized light. [7] and [8] detected the polarized mid-infrared emission (12.4 μm) of ionized Minispiral filaments, which corresponds to the thermal emission of elongated dust grains aligned along the magnetic field lines that are approximately parallel to the bulk streaming motion of the Minispiral gas. This indicates that the magnetic field with the strength of $\gtrsim 2$ mG is an inherent property of the sheared ionized gas of the Minispiral. [188] confirmed that the mid-infrared polarization is a general property of the diffused ionized gas in the Galactic center. They found the highest polarization degree of $\sim$ 12% at 12.5 μm in the Northern Arm. The polarized emission of embedded bow-shock sources is generally enhanced due to the compressed magnetic field, and the polarization degree also increases from near-infrared to mid-infrared domains, which implies that thermal emission by aligned dust grains, i.e., the reprocessed UV emission of the central star, is responsible for the polarization properties [32,33]. For the most prominent bow-shock sources - such as IRS 21 and IRS 1W, the degree of polarization of the integrated infrared emission falls in the interval of $\sim$ 10–30%. This can be explained by the Mie-scattering on dust grains, whose density is enhanced in asymmetric gaseous-dusty shells surrounding the supersonic stars [60,164].

The ionized *central cavity* ends quite sharply at $\sim$ 1.5 parsecs. Its radius is determined by the ambient UV field of the nuclear star cluster, which is concentrated in the inner parsec. Further away, from about 1.5 pc to $\sim$ 3–4 parsecs, a dense ring-like circumnuclear disk (CND) is located that is composed of neutral and molecular gas and dust with the equilibrium temperature between 20 and 80 K [18,131]. The gas number density falls into the range $\sim 10^5$–$10^8\,\mathrm{cm}^{-3}$, being the densest in numerous clumps along the ring [39] that have typical sizes of $\sim$ 0.25 pc and masses of a few $10^4\,M_\odot$. The whole CND has a mass of $\sim 10^6\,M_\odot$, being about three to four orders of magnitude more massive than the Minispiral, whose ionized mass is $\sim 350\,M_\odot$ [262]. Because of its higher mass and several tens of dense clumps, it has the potential to provide the material for the in-situ star formation in the nuclear star cluster [224], though there is no evidence of ongoing star formation; most likely turbulence and magnetic field prevent most clumps from collapsing to form stars (see, e.g., [94]). The CND and the Minispiral streamers are, interestingly, not coplanar. While the Northern Arm and the Western Arc reside in nearly the same plane, which seems to be coincident with the plane of the CND, the Eastern Arm is nearly perpendicular to the [234,262]. In this regard, the Northern Arm and the Western Arc might have originated in the inner rim of the CND, where they got detached by the combined effect of photoionization and the interaction with the outflow from the nuclear star cluster. The Minispiral is, therefore, a transient, disappearing feature with a dynamical timescale of $\sim 10^4$ years. At larger distances from the Sgr A complex, there are several massive molecular clouds, such as "$+20\,\mathrm{km\,s}^{-1}$" and "$+50\,\mathrm{km\,s}^{-1}$" giant molecular clouds (see for a review [132]).

In the central cavity, dust is present and observed, not only within the Minispiral but also closer in within the S cluster, i.e., within $1'' \sim 0.04$ pc from Sgr A*. Coreless gaseous-dusty filaments within the Minispiral are characterized by warm dust with the temperature of $\sim$ 190–265 K, which was inferred based on the 12.5/20.3 μm color-temperature map [43]. In the S cluster, fast and compact dusty D or G objects with emission lines of hydrogen and helium have been identified [40,61,80,173,174] that orbit Sgr A* on eccentric orbits similar to S stars. They are characterized by the optically thick envelopes with the photospheric radius of $\sim$ 1 AU and the black-body temperature of $\sim$ 500–600 K [173], which can be attributed to the dust thermal emission. The higher temperature of dust in comparison with dusty streamers can be explained by the model of a dust-enshrouded star [254,255], i.e., an optically thick dusty shell is heated by a central star, see Fig. 2 for an illustration. Although the nature of D/G sources is disputed, the pericenter passages of G2/DSO and G1 sources can be used to put an upper limit on the dust sublimation radius around Sgr A*, $R_{\rm sub} \sim 137\,\mathrm{AU} = 3469\,r_{\rm g}$ and $R_{\rm sub} \sim 298\,\mathrm{AU} = 7577\,r_{\rm g}$ for G2/DSO and G1 pericenter distances [174,248], respectively. Because of the current low-luminous state of Sgr A*, it can be shown that dust can approach Sgr A* within the innermost 100 gravitational radii if it is not destroyed before in shocks and by the UV

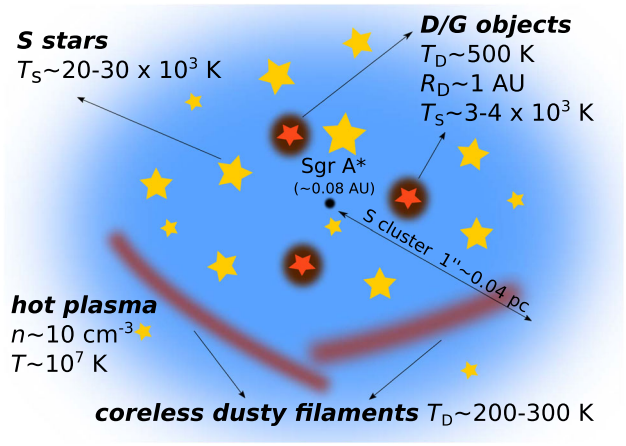

Fig. 2 Illustration of the central region of the Milky Way (S-cluster, $1'' \sim 0.04$ pc). Dust-embedded D/G sources are characterized by a higher dust temperature of ~ 500 K with the photospheric radius of $R_D \sim 1$ AU, while the coreless Minispiral streamers have a dust temperature of $\sim$ 200–300 K. The main-sequence stars within the S-cluster are predominantly of spectral type B with the effective temperature of 20–30 $\times 10^3$ K. The entire region of the Galactic center is filled with optically thin, X-ray emitting plasma with the number density of $n \sim 10\,\mathrm{cm}^{-3}$ and $T \sim 10^7$ (the figure redrawn from [173])

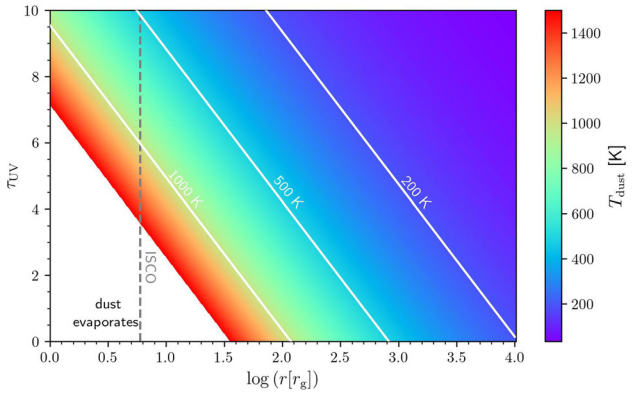

Fig. 3 Color-coded dust temperature distribution as a function of the distance r (in gravitational radii) from a low-luminosity galactic nucleus and the UV optical depth τ_{UV}. The calculation considers the central source UV luminosity of $L_{UV} = 100\,L_\odot$. The white region depicts the dust evaporation zone. The gray dashed vertical line stands for the location of the innermost stable circular orbit (ISCO) around a Schwarzschild black hole ($6\,r_g$). White solid lines represent the dust temperature of 200, 500, and 1000 K

emission of numerous OB stars. However, it cannot approach or form and linger as close as the innermost stable circular orbit if it is not shielded. We estimate the corresponding sublimation radius r_{sub} for graphite dust following [14], assuming the sublimation temperature of $T_{sub} \approx 1500$ K, the zero optical depth $\tau_{UV} = 0$, and the UV luminosity of Sgr A* with the upper limit given by its current bolometric luminosity $L_{UV} \lesssim L_{bol} \approx 100\,L_\odot$ [130]. The sublimation radius scaled to the gravitational radius can then be expressed as

$$\frac{r_{sub}}{r_g} = 38.07 \left[\left(\frac{L_{UV}}{100\,L_\odot} \right) \exp\left(-\tau_{UV}\right) \right]^{\frac{1}{2}} \left(\frac{T_{sub}}{1500\,\mathrm{K}} \right)^{-2.8} \left(\frac{M_\bullet}{4 \times 10^6\,M_\odot} \right)^{-1} . \quad (4)$$

The distribution of dust temperature T_{dust} up to the sublimation temperature of 1500 K as a function of the distance from Sgr A* (in gravitational radii) is plotted in Fig. 3, following the simple model of [14] that takes into account only the central luminosity source. We consider the optical depth in the range $\tau_{UV} \in (0, 10)$ and the UV luminosity of Sgr A* $L_{UV} = 100\,L_\odot$, which is approximately achieved during daily infrared/X-ray flares (see, e.g., [253]). It is clear that dust cannot exist close to the innermost stable orbit (dashed gray vertical line for a non-rotating black hole; $6\,r_g$) unless it is shielded by an optically thick envelope. Conditions for the survival of the clouds drifting in/out or forming in changing conditions are more complex since then the cooling timescales must be included (e.g., [25,190,191]).

Overall, the Galactic center stands for a unique environment where in the gravitational sphere of influence of the supermassive black hole (~ 2 pc) one can detect cold and dense molecular gas ($T \sim 50$ K and $n \sim 10^8\,\mathrm{cm}^{-3}$) as well as plasma close to Sgr A* that is dense and hot ($T \sim 10^{10}$ K and $n \sim 10^7\,\mathrm{cm}^{-3}$). At intermediate scales of ~ 0.1–1 pc, warm ($\sim 10^4$ K) and hot gas phases ($\sim 10^7$ K) coexist in the Minispiral region alongside the warm dust with the temperature of a few 100 K. Unfortunately, we do not have this high-resolution multi-wavelength images of other AGN.

6 Nuclear dust properties in AGN from spectral and time delay studies

In highly accreting objects, the total emission is dominated by the optical/UV radiation from the cold disk, and there is an additional bump in the near-IR [154] which comes from the dust reprocessing [14,73,178]. The basic geometry was set by the discovery of [10], but subsequent spectral studies shed more light onto the dust content, including the chemical composition.

The properties of dust are the subject of vigorous studies for a long time. The dust chemistry is very complex (see for reviews [120,123,184]). Observations reveal spectral (mostly silicate) features in emission (e.g., [89,202]) and in absorption (e.g., [6,187,229]), depending on the viewing angle in each specific source. Polycyclic Aromatic Hydrocarbons (PAH), well observed in the interstellar medium are frequently weak or not visible in AGN since they are most likely destroyed by shocks (e.g., [251,259]). The extinction curve that should be used to correct the intrinsic spectra of AGN with a certain level of extinction is still an open issue.

The standard extinction curve from the Milky Way [36] cannot be applied since the 2175 Å feature is generally not observed, but various specific shapes were proposed (e.g., [47,77,78]). This would favor amorphous carbon grains. In some objects, however, the 2175 Å feature seems to be present (in FeLoBAL objects [260]).

As discussed in Sect. 2, dust has to be concentrated in some form of a torus-like geometrical structure that is responsible for obscuring the inner parts of the nucleus in type 2 sources, while not being an obstacle blocking the view of the black hole region in type 1 sources (despite that it contributes to the IR band). Statistically, the fraction of the sky covered by the torus is thus responsible for the ratio of type 1 to type 2 sources. In a given source, the ratio of the UV emission to the IR emission also contains information about the angular extension of the dust or the covering factor (e.g., [86,121]).

Some constraints for the dust location came first from the simple consideration of the dust sublimation temperature [14,149]. The subsequent reverberation measurements (RM) of IR emission time delays with respect to the optical emission gave more specific constraints (e.g., [87,112,159]). The distance of the dusty emitters from the central black hole is effectively by a factor of 5 larger than the distance of the BLR, as determined from RM. The dust distance in a given source responds to the changes of the radiation flux, and as suggested by the data for the source NGC 4151, the recovery of the dust after the episode of a high luminosity state of the source takes a few years [160].

A novel and interesting method to localize the dust region in the equatorial plane was proposed by [197]. The method is based on reverberation measurement of the broad emission lines in polarized light in unobscured objects. For the studied source Mrk 6, they found that the size of the scattering region is around 100 light days. That is significantly smaller than the dusty region size estimated by the infrared interferometric observations.

The dusty torus localized around the equatorial plane is a key element of the AGN unification scheme, as mentioned in Sect. 2. Its evolution with redshift is the main element in cosmological applications, as the average viewing angle of AGN depends on the average opening angle of the shielding torus (see, e.g., the discussion in [181]). It is also important for all population studies of AGN. Therefore, the measurements of the correlations of the torus covering factor (or opening angle) are pursued. It seems that, for AGN with the bolometric luminosity larger than 10^{44} erg s^{-1}, no trends are seen with the luminosity or redshift (e.g., [153,181,211]). At lower luminosities, the torus seems to disappear, as discussed in Sect. 2.

7 Problems with the standard torus model and development of the most recent models

The simple idea of an AGN torus, as originally introduced by [10] and presented in numerous reviews of AGN structure, geometrical relations, and physical properties (e.g., [231]) is naturally a simplification. Firstly, a stationary torus shape cannot be supported just by thermal motions. It needs some sort of dynamical structure (inflow or outflow); a wind outflow seems to be the most likely option, and it was elaborated in numerous papers (e.g., [53,54,63,74,111]). As we now know from detailed spectral modeling, the torus has to be clumpy; otherwise, the broad band spectrum and the absorption/emission features cannot be explained [149,150,203,210].

High-resolution spatial observations reveal another problem. The original expectations were such that the high-resolution IR maps will show predominantly the dusty/molecular torus. However, the images brought us a surprise: a lot of dust emission actually came from the structure elongated in the direction of the symmetry axis. For example, [93] performed interferometric mapping of the unobscured (type 1) AGN in NGC 3783. Fitting the visibility plane, they have reached the following conclusion: most of the (mid-IR) emission comes from the polar direction. Specifically, the ratio of the polar to equatorial emission in this source turned out to be a rising function of the wavelength. The polar scattering region was subsequently revealed in a number of single-dish detections (e.g., [11,12]) as well as interferometric observations [124]. Such observations have led to a picture of the dust distribution in a form of an empty cone suggested by [91]. In the cross-section, it looks like a narrow stream of escaping dusty material, with a launching radius at the usual location of the beginning of the torus, i.e., about 1 pc from the black hole. Recently developed codes for the radiative transfer combine the disk and polar emitters. These are able to explain the observational data very well (e.g., [212,213]). Moreover, a clumpy disk with the wind models provides the best fits for the nuclear IR spectral energy distributions of partially obscured Seyfert galaxies [75].

Present-day advanced computations include the hydrodynamical simulations combined with the effects of radiation pressure. These models reveal the complexity of the medium, not just the dynamics of the outflow but also the role of convection and of complex vertical stratification (e.g., [53,55]). Magnetic fields can also play a significant role [52], as well as the torus self-gravity [102,201].

The outer disk/torus eventually overlaps with the interstellar medium and possibly also stars that naturally belong to the circumnuclear environment. Star formation in the outer parts of self-gravitating disks leads to supernovae eruptions that are capable of launching strong winds, as proposed by [41]. The medium there is clearly clumpy and dynamic. Only the most recent hydrodynamical models start to address this issue in a realistic manner (e.g., [235,246]). Such outflows clearly affect the host beyond the central parsec, and they enrich the interstellar medium with heavy elements.

8 Dust within the Broad Line Region and the FRADO model

The standard unification scheme locates the dust much farther away than the BLR. However, the possible presence of dust in the broad-line regions of AGN has been debated for many years [82]. It is well known that the ratios of the broad hydrogen Balmer emission lines are not consistent with simple predictions, and the potential presence of dust can contribute to the resolution of this issue (e.g., and the references therein [97]). Medium fully exposed to the central flux cannot retain dust at a distance smaller than the torus inner radius, but the disk in AGN is geometrically thin, and its inner part—or winds—may, in addition, shield the disk. This would allow for the dust survival close in.

Interesting measurements of the time lag between the non-polarized continuum and the polarized broad line variability in the Mrk 6 implied the presence of a scatterer residing much closer than the torus but further away than the BLR [198].

It is also a matter of fact that broad lines appear in coexistence with a cold disk located much more centrally than the torus, where the effective temperature of the accretion disk drops below the order of 1000 K, which implies the formation of low ionized dusty medium (see [47,125]). This is the basis of a model developed by [46] based on the dust-driving mechanism in which the radiation pressure of the disk is responsible for the formation of a low-ionized BLR due to the radiative acceleration of dust. The model predicts the formation of failed winds through frequent elevation of the dusty environs, illuminated by the intense central disk radiation. The subsequent fallback of dustless material occurs onto the disk: Failed Radiatively Accelerated Dusty Outflow (FRADO). The dust-driving mechanism provides an attractive, theory-motivated explanation of a natural source of low ionized broad emission lines. The scheme is supported by the measured time delays [85,167,175,237,257]. These authors have shown that Low Ionization Lines (LIL), such as Hβ and MgII, originate from a cooler and denser medium located farther with respect to the central black hole compared to the other population of broad emission lines, i.e., High Ionization Lines (HIL) such as CIV and HeII for which the line-driving mechanism is favored [139,182,240].

The new advanced numerical 2.5D FRADO computations opened up a window to the dynamical modeling of low-ionized sections of BLR. Firstly, preliminary tests showed that the 2.5D model can explain the observed location and dispersion in the radius-luminosity relation based on the reverberation-known position of the LIL BLR [22,23,176], on the basis of accretion rate [141]. Moreover, the 2.5D FRADO pictures a rather complex pattern of motions [140,142], strongly depending on the global parameters: the accretion rate, the black hole mass, and also the metallicity of material. For small values of black hole mass and accretion rate, this pattern resembles the model of a static, puffed-up disk [16] with some level of turbulence. Otherwise, an outflow structure forms similar to the one proposed by [64] and [91]. Metallicity amplifies the radiative force and intensifies the outflow for the same parameters of accretion rate and black hole mass. This mechanism manifests itself in the shape of broad emission lines [140].

[91] proposes an outflow structure initiated at radii typical for the onset of the torus (of around 10–100 times the predictions of 2.5D FRADO), thus representing the torus as a separate nested structure. On the other hand, there are studies indicating a likely connection between the BLR and the torus. The ample amount of dust of high column density extending from the equatorial plane to high altitudes and obscuring the central disk at high inclinations [10] implies a very dynamical torus structure, as already mentioned in Sect. 7. Moreover, the systematic study of the absorption events caused by the dusty clouds [126] may entail the BLR and torus as overlapping structures. A combination of the above-mentioned hints suggests that the BLR and the dusty torus are closely interrelated rather than separate identities [238]. Last but not least, the dust geometry proposed recently on the basis of the observational data (e.g., [64,81,104,105,208]) is consistent with the outflow structure in the theoretically motivated 2.5D FRADO scheme [140,142].

9 Dust scenario in Changing Look AGN

In the standard unification scheme, the AGN type is determined for a given source by its viewing angle; therefore, it should not vary. Also, in X-rays, the amount of obscuration towards the nucleus in a given source should be set by geometry and remain unchanged. However, examples of drastic changes of the X-ray obscuration [128] and of appearance and disappearance of the broad lines in some sources were reported [9]. Such objects are now referred to as Changing Look AGN (CL AGN) phenomenon. The effect was considered rather rare in the past; however, as a result of follow-up detections the sample has recently grown (e.g., [83,170,252]).

Two different physical scenarios have been tested to explain spectral and luminosity changes in CL AGN: the obscuration mechanism and the variation in the accretion state. In fact, most of the changing-look phenomena seem to be caused by accretion variation rather than a variable obscurer. The temporary obscuration or intrinsic dimming scenarios were also tested using spectropolarimetry since a low level of polarization argues against the obscuration scenario [95]. [118] discussed different obscuration scenarios for CL AGN SDSS J015957.64+003310.5., which was reported as the first CL QSO. Tentative obscuration scenarios consider the dust transported from the area of the torus that could cover the BLR emission or the processes of enhanced dust formation. However, for both scenarios, the timescales are longer than the observed changes. Timescales disagreement is the most robust argument

for most CL AGNs against the obscuration scenario. The possible presence of the dust within BLR and the atypical extinction properties of AGN dust may open some paths to use obscuration as a plausible CL mechanism. In the case of intrinsic changes, timescales are also much shorter than normal viscous timescales in the standard accretion disks, and appropriate model modifications have to be made to accommodate the observational data (e.g., [103,166,204,206]). Further studies are clearly needed.

10 Dust origin in AGN

Dust in the BLR and in the dusty/molecular torus can either come from the interstellar medium, or it can form *in situ*. The correct answer is currently unclear. The solar and frequently super-solar metallicity, even at high redshift quasars, is not consistent with the expected low metallicity of the high redshift galaxies (see, e.g., and further references therein [169,205]). On the other hand, vigorous star formation actually precedes the quasar activity, and multiple supernovae in the circumnuclear stellar cluster creating heavy elements enrich the material that later accretes (see for the most recent plot of the history of star formation rate and of quasar activity [72]).

The *in situ* option is interesting. Outer parts of the disk can be gravitationally unstable, leading to vigorous star-forming, with predominantly fast-evolving massive stars (e.g., [35,100]). What is more, the standard disk in the region of the effective temperature ~ 1500 K allows the formation of dust directly in the disk atmosphere, in a similar way as in stars, and this mechanism was already discussed by [65].

Local production can possibly supply the dust much faster than the external source if dust is temporarily destroyed during the bright stage of an AGN, although more studies of this issue similar to the tentative reports by [160] are needed.

11 Summary

The presence of the dust in AGN is well known from the spectroscopic studies done back in the 1960 s and 1970 s (see and the references therein [161]). Over the years, there has been gradual progress in our knowledge of the dust location and distribution that came from polarimetric studies, interferometric measurements in the IR, and time-domain measurements. We understand the role of dust in the AGN classification scheme, and we have an insight into the dynamics of this complex, clumpy region. However, there are still important unresolved questions related to the formation of the dusty region and its connection with the host galaxy.

The most important problem is the relation of the dust to the accretion disk. It may seem that the absence of the cold disk and the presence of the exclusively hot flow prevents the existence of the BLR and of the dusty torus. However, such a hypothesis is not proven observationally, and it is not easy to test it since, at a fraction of a parsec, the presence of the disk overlapping with BLR and torus region is hard to resolve. The polarization-based arguments of the decomposition of quasar spectra support the idea of the cold disk underlying the two regions [107]. The progress in IR interferometric studies will certainly shed light on the exact geometry of the dust close to the dust sublimation radius (see, e.g., for one of the most recent results for NGC 4151 [108]). Such values done for more objects, and possibly in the same object repeated after a few years, can help us to understand the evolutionary aspects.

Interesting new developments are now coming from the James Webb Space Telescope (JWST) launched at the end of 2021. Indeed, one of the four general aims of JWST is to trace the process of the assembly of galaxies. Since AGN is an important stage in a galaxy's life, it will also shed light on the growth of the central black hole and the feeding and feedback. Dusty outflows in AGN are massive so they are an important element of the overall puzzle. We thus, expect a lot of new developments in dust formation and dust circulation in galaxies, including their AGN phase. Infrared observations give a direct insight into star formation in dusty galaxies, including the interacting galaxies (e.g., [66]). Particular attention is paid to extremely red quasars, with bolometric luminosity exceeding 10^{47} erg s^{-1} at high redshift (e.g., [250]). Sources like the one studied in this paper (SDSS J165202.64+172852.3) reveal the formation stage of the core of the clusters of galaxies. These are excellent candidates for super-Eddington accretion important to explain the fast rise of the black hole mass from the initial seeds that are required to match the observed distribution of the black hole masses [98,225]. It also allows to map of the inner ~ 1 kpc of nearby AGN with the resolution of ~ 100 pc and sheds light on the circumnuclear starburst ring and the associated outflow (e.g., [230]). Such observations allow us to quantify the vigorously discussed issue of the feedback of an active nucleus to the host as well as the feeding pattern of the central black hole.

Acknowledgements This project has received funding from the European Research Council (ERC) under the European Union's Horizon 2020 research and innovation program (Grant Agreement No. [951549]). The project was partially supported by the Polish Funding Agency National Science Centre, project 2017/26/A/ST9/00756 (MAESTRO 9), and MNiSW grant DIR/WK/2018/12. MLM-A acknowledges financial support from Millennium Nucleus NCN19_058 (TITANs). VK acknowledges the Czech Science Foundation Project No. 21-06825X "Accreting black holes in the new era of X-ray polarimetry missions". SP acknowledges financial support from the Conselho Nacional de Desenvolvimento Científico e Tecnológico (CNPq) Fellowship (164753/2020-6). MS acknowledges the financial support of the Polish Funding Agency National Science Centre 2021/41/N/ST9/02280 (PRELUDIUM 20). MZ acknowl-

edges the financial support of the GAČR EXPRO Grant No. 21-13491X "Exploring the Hot Universe and Understanding Cosmic Feedback". The authors also acknowledge the Czech-Polish mobility program (MŠMT 8J20PL037 and NAWA PPN/BCZ/2019/1/00069), the OPUS-LAP/GAČR-LA bilateral project (UMO-2021/43/I/ST9/01352 and GF22-04053 L), and the Czech Ministry of Education, Youth and Sports Research Infrastructure (LM2023047).

Author contributions

All authors contributed to the study's conception and design. BC was the leading author in writing the text. MZ, MHN, MS, SP and VK wrote some parts of the text. TPA provided a better version of Fig. 1. SP and VKJ helped considerably with text formatting. MS and MLM-A provided a number of references. All authors sent their comments to the first draft. Finally, all authors carefully reviewed and approved the final version of the text.

Funding The funding details are listed in the Acknowledgement section.

Data Availability Statement This manuscript has no associated data or the data will not be deposited. [Authors' comment: Data sharing not applicable to this article as no datasets were generated or analyzed during the current study.]

Declarations

Conflict of interest The authors declare they have no financial interests.

Code availability Codes can be available on request.

Ethical approval Not applicable.

Consent to participate All authors contributed to the work and approved sending the paper for publication.

Consent for publication All authors agree for the work to be published in the European Physical Journal D, Topical Issue: "Physics of Ionized Gases and Spectroscopy of Isolated Complex Systems: Fundamentals and Applications".

References

1. M.A. Abramowicz, B. Czerny, J.P. Lasota et al., Slim accretion disks. Astrophys. J. **332**, 646 (1988). https://doi.org/10.1086/166683
2. M.A. Abramowicz, X. Chen, S. Kato et al., Thermal Equilibria of Accretion Disks. ApJ **438**, L37 (1995). https://doi.org/10.1086/187709. arXiv:astro-ph/9409018 [astro-ph]
3. T.P. Adhikari, A. Różańska, M. Sobolewska et al., Absorption measure distribution in Mrk 509. ApJ **815**(2), 83 (2015). https://doi.org/10.1088/0004-637X/815/2/83. arXiv:1507.04035 [astro-ph.GA]
4. T.P. Adhikari, A. Różańska, B. Czerny et al., The intermediate-line region in active galactic nuclei. ApJ **831**(1), 68 (2016). https://doi.org/10.3847/0004-637X/831/1/68. arXiv:1606.00284 [astro-ph.GA]
5. T.P. Adhikari, A. Różańska, K. Hryniewicz et al., What shapes the absorption measure distribution in AGN outflows? ApJ **881**(1), 78 (2019). https://doi.org/10.3847/1538-4357/ab2dfc. arXiv:1812.05154 [astro-ph.GA]
6. D.K. Aitken, P.F. Roche, 8–13 mu-m spectrophotometry of galaxies - IV. Six more Seyferts and 3C 345. MNRAS **213**, 777–788 (1985). https://doi.org/10.1093/mnras/213.4.777
7. D.K. Aitken, D. Gezari, C.H. Smith et al., Polarimetric imaging of the galactic center at 12.4 microns: the detailed magnetic field structure in the Northern arm and east-west bar. ApJ **380**, 419 (1991). https://doi.org/10.1086/170600
8. D.K. Aitken, C.H. Smith, T.J.T. Moore et al., Mid-infrared polarization studies of SgrA: a three-dimensional study of the central parsec. MNRAS **299**(3), 743–752 (1998). https://doi.org/10.1046/j.1365-8711.1998.01807.x
9. D. Alloin, D. Pelat, M. Phillips et al., Recent spectral variations in the active nucleus of NGC 1566. ApJ **288**, 205–220 (1985). https://doi.org/10.1086/162783
10. R.R.J. Antonucci, J.S. Miller, Spectropolarimetry and the nature of NGC 1068. ApJ **297**, 621–632 (1985). https://doi.org/10.1086/163559
11. D. Asmus, New evidence for the ubiquity of prominent polar dust emission in AGN on tens of parsec scales. MNRAS **489**(2), 2177–2188 (2019). https://doi.org/10.1093/mnras/stz2289. arXiv:1908.03552 [astro-ph.GA]
12. D. Asmus, S.F. Hönig, P. Gandhi, The subarcsecond mid-infrared view of local active galactic nuclei. III. Polar dust emission. ApJ **822**(2), 109 (2016). https://doi.org/10.3847/0004-637X/822/2/109. arXiv:1603.02710 [astro-ph.GA]
13. F.K. Baganoff, Y. Maeda, M. Morris et al., Chandra X-ray spectroscopic imaging of sagittarius A* and the central parsec of the galaxy. ApJ **591**(2), 891–915 (2003). https://doi.org/10.1086/375145. arXiv:astro-ph/0102151 [astro-ph]
14. R. Barvainis, Hot dust and the near-infrared bump in the continuum spectra of quasars and active galactic

nuclei. ApJ **320**, 537 (1987). https://doi.org/10.1086/165571
15. A. Baskin, A. Laor, What controls the [OIII]λ5007 line strength in active galactic nuclei? MNRAS **358**(3), 1043–1054 (2005). https://doi.org/10.1111/j.1365-2966.2005.08841.x. arXiv:astro-ph/0501436 [astro-ph]
16. A. Baskin, A. Laor, Dust inflated accretion disc as the origin of the broad line region in active galactic nuclei. MNRAS **474**(2), 1970–1994 (2018). https://doi.org/10.1093/mnras/stx2850. arXiv:1711.00025 [astro-ph.GA]
17. A. Baskin, A. Laor, Radiation pressure confinement - V. The predicted free-free absorption and emission in active galactic nuclei. MNRAS **508**(1), 680–697 (2021). https://doi.org/10.1093/mnras/stab2555. arXiv:2109.03313 [astro-ph.GA]
18. E.E. Becklin, I. Gatley, M.W. Werner, Far-infrared observations of Sagittarius A-the luminosity and dust density in the central parsec of the galaxy. ApJ **258**, 135–142 (1982). https://doi.org/10.1086/160060
19. M.C. Begelman, C.F. McKee, Global effects of thermal conduction on two-phase media. ApJ **358**, 375 (1990). https://doi.org/10.1086/168994
20. A.M. Beloborodov, Accretion Disk Models. In: Poutanen J, Svensson R (eds) High Energy Processes in Accreting Black Holes, p 295, (1999) https://doi.org/10.48550/arXiv.astro-ph/9901108, arXiv:astro-ph/9901108
21. N. Bennert, B. Jungwiert, S. Komossa et al., Size and properties of the narrow-line region in Seyfert-1 galaxies from spatially-resolved optical spectroscopy. A&A **459**(1), 55–69 (2006). https://doi.org/10.1051/0004-6361:20065477. arXiv:astro-ph/0606367 [astro-ph]
22. M.C. Bentz, J.L. Walsh, A.J. Barth et al., The lick AGN monitoring project: broad-line region radii and black hole masses from reverberation mapping of Hβ. ApJ **705**(1), 199–217 (2009). https://doi.org/10.1088/0004-637X/705/1/199. arXiv:0908.0003 [astro-ph.CO]
23. M.C. Bentz, K.D. Denney, C.J. Grier et al., The low-luminosity end of the radius-luminosity relationship for active galactic nuclei. ApJ **767**(2), 149 (2013). https://doi.org/10.1088/0004-637X/767/2/149. arXiv:1303.1742 [astro-ph.CO]
24. M. Berton, E. Järvelä, Jet-induced feedback in the [O III] lines of early evolution stage active galactic nuclei. Universe **7**(6), 188 (2021). https://doi.org/10.3390/universe7060188. arXiv:2106.01076 [astro-ph.GA]
25. H.K. Bhat, N.B. Sabha, M. Zajaček et al., Mid-infrared studies of dusty sources in the galactic center. ApJ **929**(2), 178 (2022). https://doi.org/10.3847/1538-4357/ac6106. arXiv:2203.16727 [astro-ph.GA]
26. S. Bianchi, R. Antonucci, A. Capetti et al., HST unveils a compact mildly relativistic broad-line region in the candidate true type 2 NGC 3147. MNRAS **488**(1), L1–L5 (2019). https://doi.org/10.1093/mnrasl/slz080. arXiv:1905.09627 [astro-ph.HE]
27. S. Bianchi, M. Chiaberge, A. Laor et al., NGC 3147: a prototypical low-luminosity active galactic nucleus with double-peaked optical and ultraviolet lines. MNRAS **516**(4), 5775–5784 (2022). https://doi.org/10.1093/mnras/stac2290. arXiv:2209.01807 [astro-ph.HE]
28. S. Bianchi, V. Mainieri, P. Padovani, Active Galactic Nuclei and their demography through cosmic time. (2022b) arXiv e-prints https://doi.org/10.48550/arXiv.2203.16846, arXiv:2203.16846 [astro-ph.HE]
29. R.C. Bohlin, B.D. Savage, J.F. Drake, A survey of interstellar H I from Lalpha absorption measurements. II. ApJ **224**, 132–142 (1978). https://doi.org/10.1086/156357
30. H. Bondi, On spherically symmetrical accretion. MNRAS **112**, 195 (1952). https://doi.org/10.1093/mnras/112.2.195
31. A. Borkar, T.P. Adhikari, A. Różańska et al., The multiphase environment in the centre of Centaurus A. MNRAS **500**(3), 3536–3551 (2021). https://doi.org/10.1093/mnras/staa3515. arXiv:2006.01099 [astro-ph.GA]
32. R.M. Buchholz, G. Witzel, R. Schödel et al., Adaptive-optics assisted near-infrared polarization measurements of sources in the Galactic center. A&A **534**, A117 (2011). https://doi.org/10.1051/0004-6361/201117300. arXiv:1107.3781 [astro-ph.GA]
33. R.M. Buchholz, G. Witzel, R. Schödel et al., Ks- and Lp-band polarimetry on stellar and bow-shock sources in the Galactic center. A&A **557**, A82 (2013). https://doi.org/10.1051/0004-6361/201220338. arXiv:1308.0956 [astro-ph.GA]
34. D. Calzetti, L. Armus, R.C. Bohlin et al., The dust content and opacity of actively star-forming galaxies. ApJ **533**(2), 682–695 (2000). https://doi.org/10.1086/308692. arXiv:astro-ph/9911459 [astro-ph]
35. M. Cantiello, A.S. Jermyn, D.N.C. Lin, Stellar evolution in AGN disks. ApJ **910**(2), 94 (2021). https://doi.org/10.3847/1538-4357/abdf4f. arXiv:2009.03936 [astro-ph.SR]
36. J.A. Cardelli, G.C. Clayton, J.S. Mathis, The relationship between infrared, optical, and ultraviolet extinction. ApJ **345**, 245 (1989). https://doi.org/10.1086/167900
37. L. Chevallier, B. Czerny, A. Róańska et al., Response of the warm absorber cloud to a variable nuclear flux in active galactic nuclei. A&A **467**(3), 971–978 (2007). https://doi.org/10.1051/0004-6361:20065657. arXiv:astro-ph/0701112 [astro-ph]
38. H. Choi, K.M. Leighly, D.M. Terndrup et al., The physical properties of low-redshift FeLoBAL quasars. I. Spectral-synthesis analysis of the broad absorption-line (BAL) outflows using SimBAL. ApJ **937**(2), 74 (2022). https://doi.org/10.3847/1538-4357/ac61d9. arXiv:2203.11964 [astro-ph.GA]
39. M.H. Christopher, N.Z. Scoville, S.R. Stolovy et al., HCN and HCO^+ observations of the Galactic circumnuclear disk. ApJ **622**(1), 346–365 (2005). https://doi.org/10.1086/427911. arXiv:astro-ph/0502532 [astro-ph]
40. A. Ciurlo, R.D. Campbell, M.R. Morris et al., A population of dust-enshrouded objects orbiting the Galactic black hole. Nature **577**(7790), 337–340 (2020). https://doi.org/10.1038/s41586-019-1883-y. arXiv:2001.08325 [astro-ph.GA]

41. S. Collin, J.P. Zahn, Star formation and evolution in accretion disks around massive black holes. A&A **344**, 433–449 (1999)
42. S. Collin-Souffrin, Line and continuum radiation from the outer region of accretion discs in active galactic nuclei. I-Preliminary considerations. A&A **179**(1–2), 60–70 (1987)
43. A. Cotera, M. Morris, A.M. Ghez, et al. Mid-Infrared Imaging of the Central Parsec with Keck. In: Falcke H, Cotera A, Duschl WJ, et al (eds) The Central Parsecs of the Galaxy, p 240 (1999)
44. B. Czerny, M. Elvis, Constraints on Quasar Accretion Disks from the Optical/Ultraviolet/Soft X-Ray Big Bump. Astrophys. J. **321**, 305 (1987). https://doi.org/10.1086/165630
45. B. Czerny, M. Elvis, Constraints on quasar accretion disks from the optical/ultraviolet/soft X-ray big bump. ApJ **321**, 305 (1987). https://doi.org/10.1086/165630
46. B. Czerny, K. Hryniewicz, The origin of the broad line region in active galactic nuclei. A&A **525**, L8 (2011). https://doi.org/10.1051/0004-6361/201016025. arXiv:1010.6201 [astro-ph.CO]
47. B. Czerny, J. Li, Z. Loska et al., Extinction due to amorphous carbon grains in red quasars from the Sloan Digital Sky Survey. MNRAS **348**(3), L54–L57 (2004). https://doi.org/10.1111/j.1365-2966.2004.07590.x. arXiv:astro-ph/0401158 [astro-ph]
48. B. Czerny, A. Różańska, J. Kuraszkiewicz, Constraints for the accretion disk evaporation rate in AGN from the existence of the Broad Line Region. A&A **428**, 39–49 (2004b). https://doi.org/10.1051/0004-6361:20040487. arXiv:astro-ph/0403507 [astro-ph]
49. R.C. Dannen, D. Proga, T. Waters et al., Clumpy AGN outflows due to thermal instability. ApJ **893**(2), L34 (2020). https://doi.org/10.3847/2041-8213/ab87a5. arXiv:2001.00133 [astro-ph.GA]
50. M. de Laurentis, I. De Martino, R. Della Monica, The Galactic Center as a laboratory for theories of gravity and dark matter (2022) . arXiv e-prints arXiv:2211.07008
51. C. Done, S.W. Davis, C. Jin et al., Intrinsic disc emission and the soft X-ray excess in active galactic nuclei. MNRAS **420**(3), 1848–1860 (2012). https://doi.org/10.1111/j.1365-2966.2011.19779.x. arXiv:1107.5429 [astro-ph.HE]
52. A. Dorodnitsyn, T. Kallman, Parsec-scale obscuring accretion disk with large-scale magnetic field in AGNs. ApJ **842**(1), 43 (2017). https://doi.org/10.3847/1538-4357/aa7264. arXiv:1705.03975 [astro-ph.GA]
53. A. Dorodnitsyn, T. Kallman, A physical model for a radiative. Convective dusty disk in AGN. ApJ **910**(1), 67 (2021). https://doi.org/10.3847/1538-4357/abe121. arXiv:2007.06572 [astro-ph.GA]
54. A. Dorodnitsyn, T. Kallman, D. Proga, An axisymmetric, hydrodynamical model for the torus wind in active Galactic nuclei. ApJ **675**(1), L5 (2008). https://doi.org/10.1086/529374. arXiv:0801.1470 [astro-ph]
55. A. Dorodnitsyn, T. Kallman, G.S. Bisnovatyi-Kogan, AGN obscuration through dusty, infrared-dominated flows. II. Multidimensional. Radiation-hydrodynamics modeling. ApJ **747**(1), 8 (2012). https://doi.org/10.1088/0004-637X/747/1/8. arXiv:1111.2103 [astro-ph.HE]
56. B.T. Draine, Interstellar dust grains. ARA&A **41**, 241–289 (2003). https://doi.org/10.1146/annurev.astro.41.011802.094840. arXiv:astro-ph/0304489 [astro-ph]
57. B.T. Draine, E.E. Salpeter, Destruction mechanisms for interstellar dust. ApJ **231**, 438–455 (1979). https://doi.org/10.1086/157206
58. B.T. Draine, E.E. Salpeter, On the physics of dust grains in hot gas. ApJ **231**, 77–94 (1979). https://doi.org/10.1086/157165
59. B.T. Draine, E.E. Salpeter, On the physics of dust grains in hot gas. ApJ **231**, 77–94 (1979). https://doi.org/10.1086/157165
60. A. Eckart, R. Genzel, R. Hofmann et al., High angular resolution spectroscopic and polarimetric imaging of the Galactic center in the near-infrared. ApJ **445**, L23 (1995). https://doi.org/10.1086/187880
61. A. Eckart, K. Mužić, S. Yazici et al., Near-infrared proper motions and spectroscopy of infrared excess sources at the Galactic center. A&A **551**, A18 (2013). https://doi.org/10.1051/0004-6361/201219994. arXiv:1208.1907 [astro-ph.IM]
62. A. Eckart, A. Hüttemann, C. Kiefer et al., The Milky Way's supermassive black hole: How good a case is it? Found. Phys. **47**(5), 553–624 (2017). https://doi.org/10.1007/s10701-017-0079-2. arXiv:1703.09118 [astro-ph.HE]
63. M. Elitzur, I. Shlosman, The AGN-obscuring torus: The end of the "Doughnut" paradigm? ApJ **648**(2), L101–L104 (2006). https://doi.org/10.1086/508158. arXiv:astro-ph/0605686 [astro-ph]
64. M. Elvis, A structure for quasars. Astrophys. J. **545**(1), 63–76 (2000). https://doi.org/10.1086/317778. arXiv:astro-ph/0008064 [astro-ph]
65. M. Elvis, M. Marengo, M. Karovska, Smoking quasars: a new source for cosmic dust. ApJ **567**(2), L107–L110 (2002). https://doi.org/10.1086/340006. arXiv:astro-ph/0202002 [astro-ph]
66. A.S. Evans, D.T. Frayer, V. Charmandaris et al., GOALS-JWST: hidden star formation and extended PAH emission in the luminous infrared galaxy VV 114. ApJ **940**(1), L8 (2022). https://doi.org/10.3847/2041-8213/ac9971. arXiv:2208.14507 [astro-ph.GA]
67. Event Horizon Telescope. Collaboration, K. Akiyama, A. Alberdi et al., First M87 event horizon telescope results. IV. Imaging the central supermassive black hole. ApJ **875**(1), L4 (2019). https://doi.org/10.3847/2041-8213/ab0e85. arXiv:1906.11241 [astro-ph.GA]
68. K. Akiyama, A. Alberdi, Event Horizon Telescope Collaboration et al., First sagittarius A* event horizon telescope results. I. The shadow of the supermassive black hole in the center of the Milky Way. ApJ **930**(2), 12 (2022). https://doi.org/10.3847/2041-8213/ac6674
69. G.J. Ferland, M. Chatzikos, F. Guzmán et al., The 2017 release cloudy. Rev. Mexicana Astron. Astrofis. **53**, 385–438 (2017). arXiv:1705.10877 [astro-ph.GA]
70. J. Ferreira, G. Pelletier, Magnetized accretion-ejection structures. III. Stellar and extragalactic jets as weakly dissipative disk outflows. A&A **295**, 807 (1995)
71. G.B. Field, Thermal instability. ApJ **142**, 531 (1965). https://doi.org/10.1086/148317

72. F. Fiore, C. Feruglio, F. Shankar et al., AGN wind scaling relations and the co-evolution of black holes and galaxies. A&A **601**, A143 (2017). https://doi.org/10.1051/0004-6361/201629478. arXiv:1702.04507 [astro-ph.GA]
73. J. Fritz, A. Franceschini, E. Hatziminaoglou, Revisiting the infrared spectra of active galactic nuclei with a new torus emission model. MNRAS **366**(3), 767–786 (2006). https://doi.org/10.1111/j.1365-2966.2006.09866.x. arXiv:astro-ph/0511428 [astro-ph]
74. S.C. Gallagher, J.E. Everett, M.M. Abado et al., Investigating the structure of the windy torus in quasars. MNRAS **451**(3), 2991–3000 (2015). https://doi.org/10.1093/mnras/stv1126. arXiv:1505.04219 [astro-ph.GA]
75. I. García-Bernete, O. González-Martín, C. Ramos Almeida et al., Torus and polar dust dependence on active galactic nucleus properties. A&A **667**, A140 (2022). https://doi.org/10.1051/0004-6361/202244230. arXiv:2210.03508 [astro-ph.GA]
76. S. García-Burillo, F. Combes, A. Usero et al., Molecular line emission in NGC 1068 imaged with ALMA. I. An AGN-driven outflow in the dense molecular gas. A&A **567**, A125 (2014). https://doi.org/10.1051/0004-6361/201423843. arXiv:1405.7706 [astro-ph.GA]
77. C.M. Gaskell, R.W. Goosmann, R.R.J. Antonucci et al., The nuclear reddening curve for active galactic nuclei and the shape of the infrared to X-ray spectral energy distribution. ApJ **616**(1), 147–156 (2004). https://doi.org/10.1086/423885. arXiv:astro-ph/0309595 [astro-ph]
78. C.M. Gaskell, F.C., Anderson, SÁ. Birmingham, et al Estimating reddening of the continuum and broad-line region of active galactic nuclei: the mean reddening of NGC 5548 and the size of the accretion disc (2022). arXiv e-prints arXiv:2208.11437
79. R. Genzel, Nobel lecture: a forty-year journey*. Rev. Mod. Phys. **94**(2), 020501 (2022). https://doi.org/10.1103/RevModPhys.94.020501
80. S. Gillessen, R. Genzel, T.K. Fritz et al., A gas cloud on its way towards the supermassive black hole at the Galactic Centre. Nature **481**(7379), 51–54 (2012). https://doi.org/10.1038/nature10652. arXiv:1112.3264 [astro-ph.GA]
81. M.R. Goad, K.T. Korista, A.J. Ruff, The broad emission-line region: the confluence of the outer accretion disc with the inner edge of the dusty torus. MNRAS **426**(4), 3086–3111 (2012). https://doi.org/10.1111/j.1365-2966.2012.21808.x. arXiv:1207.6339 [astro-ph.CO]
82. R.W. Goodrich, Dust in the Broad-Line Regions of Seyfert Galaxies. ApJ **440**, 141 (1995). https://doi.org/10.1086/175256
83. M.J. Graham, N.P. Ross, D. Stern et al., Understanding extreme quasar optical variability with CRTS - II. Changing-state quasars. MNRAS **491**(4), 4925–4948 (2020). https://doi.org/10.1093/mnras/stz3244. arXiv:1905.02262 [astro-ph.GA]
84. G.R.A.V.I.T.Y. Collaboration, R. Abuter, A. Amorim et al., Detection of orbital motions near the last stable circular orbit of the massive black hole SgrA*. A&A **618**, L10 (2018). https://doi.org/10.1051/0004-6361/201834294. arXiv:1810.12641 [astro-ph.GA]
85. C.J. Grier, B.M. Peterson, K. Horne et al., The structure of the broad-line region in active Galactic nuclei. I. Reconstructed velocity-delay maps. ApJ **764**(1), 47 (2013). https://doi.org/10.1088/0004-637X/764/1/47. arXiv:1210.2397 [astro-ph.CO]
86. M. Gu, The evolution of the dusty torus covering factor in quasars. ApJ **773**(2), 176 (2013). https://doi.org/10.1088/0004-637X/773/2/176. arXiv:1307.1193 [astro-ph.CO]
87. E. Guise, S.F. Hönig, V. Gorjian et al., Dust reverberation mapping and light-curve modelling of Zw229-015. MNRAS **516**(4), 4898–4915 (2022). https://doi.org/10.1093/mnras/stac2529. arXiv:2209.01409 [astro-ph.GA]
88. A. Gupta, S. Mathur, Y. Krongold et al., A two-phase low-velocity outflow in the Seyfert 1 galaxy ark 564. ApJ **768**(2), 141 (2013). https://doi.org/10.1088/0004-637X/768/2/141. arXiv:1301.6138 [astro-ph.HE]
89. E. Hatziminaoglou, A. Hernán-Caballero, A. Feltre et al., A complete census of silicate features in the mid-infrared spectra of active galaxies. ApJ **803**(2), 110 (2015). https://doi.org/10.1088/0004-637X/803/2/110. arXiv:1502.05823 [astro-ph.GA]
90. T. Holczer, E. Behar, S. Kaspi, Absorption measure distribution of the outflow in IRAS 13349+2438: Direct observation of thermal instability? ApJ **663**(2), 799–807 (2007). https://doi.org/10.1086/518416. arXiv:astro-ph/0703351 [astro-ph]
91. S.F. Hönig, Redefining the torus: a unifying view of AGNs in the infrared and submillimeter. ApJ **884**(2), 171 (2019). https://doi.org/10.3847/1538-4357/ab4591. arXiv:1909.08639 [astro-ph.GA]
92. S.F. Hönig, T. Beckert, K. Ohnaka et al., Radiative transfer modeling of three-dimensional clumpy AGN tori and its application to NGC 1068. A&A **452**(2), 459–471 (2006). https://doi.org/10.1051/0004-6361:20054622. arXiv:astro-ph/0602494 [astro-ph]
93. S.F. Hönig, M. Kishimoto, K.R.W. Tristram et al., Dust in the polar region as a major contributor to the infrared emission of active Galactic nuclei. ApJ **771**(2), 87 (2013). https://doi.org/10.1088/0004-637X/771/2/87. arXiv:1306.4312 [astro-ph.CO]
94. P.Y. Hsieh, P.M. Koch, W.T. Kim et al., The circumnuclear disk revealed by ALMA. I. Dense clouds and tides in the Galactic center. ApJ **913**(2), 94 (2021). https://doi.org/10.3847/1538-4357/abf4cd. arXiv:2104.02078 [astro-ph.GA]
95. D. Hutsemékers, B. Agís González, F. Marin et al., Polarization of changing-look quasars. A&A **625**, A54 (2019). https://doi.org/10.1051/0004-6361/201834633. arXiv:1904.03914 [astro-ph.GA]
96. S. Ichimaru, Bimodal behavior of accretion disks: theory and application to Cygnus X-1 transitions. Astrophys. J. **214**, 840–855 (1977). https://doi.org/10.1086/155314
97. D. Ilić, L.Č Popović, G. La Mura et al., The analysis of the broad hydrogen Balmer line ratios: possible implications for the physical properties of the broad line region of AGNs. A&A **543**, A142 (2012). https://doi.org/10.1051/0004-6361/201219299. arXiv:1205.3950 [astro-ph.CO]
98. K. Inayoshi, E. Visbal, Z. Haiman, The assembly of the first massive black holes. ARA&A

58, 27–97 (2020). https://doi.org/10.1146/annurev-astro-120419-014455. arXiv:1911.05791 [astro-ph.GA]
99. O. Ishihara, TOPICAL REVIEW: complex plasma: dusts in plasma. J. Phys. D Appl. Phys. **40**(8), R121–R147 (2007). https://doi.org/10.1088/0022-3727/40/8/R01
100. A.S. Jermyn, A.J. Dittmann, M. Cantiello et al., Stellar evolution in the disks of active Galactic nuclei produces rapidly rotating massive stars. ApJ **914**(2), 105 (2021). https://doi.org/10.3847/1538-4357/abfb67. arXiv:2102.13114 [astro-ph.HE]
101. D. Kakkad, B. Groves, M. Dopita et al., Spatially resolved electron density in the narrow line region of z < 0.02 radio AGNs. A&A **618**, A6 (2018). https://doi.org/10.1051/0004-6361/201832790. arXiv:1806.02839 [astro-ph.GA]
102. V. Karas, J.M. Huré, O. Semerák, TOPICAL REVIEW: gravitating discs around black holes. Class. Quantum Gravity **21**(7), R1–R51 (2004). https://doi.org/10.1088/0264-9381/21/7/R01. arXiv:astro-ph/0401345 [astro-ph]
103. K. Kaur, N.C. Stone, S. Gilbaum, Magnetically Dominated Disks in Tidal Disruption Events and Quasi-Periodic Eruptions (2022). arXiv e-prints arXiv:2211.00704. [astro-ph.HE]
104. T. Kawaguchi, M. Mori, Orientation effects on the inner region of dusty torus of active Galactic nuclei. ApJ **724**(2), L183–L187 (2010). https://doi.org/10.1088/2041-8205/724/2/L183. arXiv:1010.5799 [astro-ph.CO]
105. T. Kawaguchi, M. Mori, Near-infrared reverberation by dusty clumpy tori in active Galactic nuclei. ApJ **737**(2), 105 (2011). https://doi.org/10.1088/0004-637X/737/2/105. arXiv:1107.0678 [astro-ph.CO]
106. M. Kishimoto, S.F. Hönig, T. Beckert et al., The innermost region of AGN tori: implications from the HST/NICMOS type 1 point sources and near-IR reverberation. A&A **476**(2), 713–721 (2007). https://doi.org/10.1051/0004-6361:20077911. arXiv:0709.0431 [astro-ph]
107. M. Kishimoto, R. Antonucci, O. Blaes et al., The characteristic blue spectra of accretion disks in quasars as uncovered in the infrared. Nature **454**(7203), 492–494 (2008). https://doi.org/10.1038/nature07114. arXiv:0807.3703 [astro-ph]
108. M. Kishimoto, M. Anderson, T. ten Brummelaar et al., The dust sublimation region of the type 1 AGN NGC 4151 at a hundred microarcsecond scale as resolved by the CHARA array interferometer. ApJ **940**(1), 28 (2022). https://doi.org/10.3847/1538-4357/ac91c4. arXiv:2209.06061 [astro-ph.GA]
109. W. Kollatschny, M. Zetzl, Broad-line active galactic nuclei rotate faster than narrow-line ones. Nature **470**(7334), 366–368 (2011). https://doi.org/10.1038/nature09761
110. W. Kollatschny, M. Zetzl, The shape of broad-line profiles in active galactic nuclei. A&A **549**, A100 (2013). https://doi.org/10.1051/0004-6361/201219411. arXiv:1211.3065 [astro-ph.CO]
111. A. Konigl, J.F. Kartje, Disk-driven hydromagnetic winds as a key ingredient of active Galactic nuclei unification schemes. ApJ **434**, 446 (1994). https://doi.org/10.1086/174746
112. S. Koshida, T. Minezaki, Y. Yoshii et al., Reverberation measurements of the inner radius of the dust torus in 17 seyfert galaxies. ApJ **788**(2), 159 (2014). https://doi.org/10.1088/0004-637X/788/2/159. arXiv:1406.2078 [astro-ph.GA]
113. J. Kovář, P. Slaný, Z. Stuchlík et al., Role of electric charge in shaping equilibrium configurations of fluid tori encircling black holes. Phys. Rev. **84**(8), 084002 (2011). https://doi.org/10.1103/PhysRevD.84.084002. arXiv:1110.4843 [astro-ph.HE]
114. J.H. Krolik, *Active Galactic Nuclei. From the Central Black Hole to the Galactic Environment* (Princeton University Press, Princeton, 1999)
115. J.H. Krolik, G.A. Kriss, Warm absorbers in active Galactic nuclei: a multitemperature wind. ApJ **561**(2), 684–690 (2001). https://doi.org/10.1086/323442
116. J.H. Krolik, C.F. McKee, C.B. Tarter, Two-phase models of quasar emission line regions. ApJ **249**, 422–442 (1981). https://doi.org/10.1086/159303
117. D. Kunneriath, A. Eckart, S.N. Vogel et al., The Galactic centre mini-spiral in the mm-regime. A&A **538**, A127 (2012). https://doi.org/10.1051/0004-6361/201117676. arXiv:1201.2362 [astro-ph.GA]
118. S.M. LaMassa, S. Cales, E.C. Moran et al., The discovery of the first "Changing Look" quasar: new insights into the physics and phenomenology of active Galactic nucleus. ApJ **800**(2), 144 (2015). https://doi.org/10.1088/0004-637X/800/2/144. arXiv:1412.2136 [astro-ph.GA]
119. A. Laor, On the nature of low-luminosity narrow-line active Galactic nuclei. ApJ **590**(1), 86–94 (2003). https://doi.org/10.1086/375008. arXiv:astro-ph/0302541 [astro-ph]
120. A. Laor, B.T. Draine, Spectroscopic constraints on the properties of dust in active Galactic nuclei. ApJ **402**, 441 (1993). https://doi.org/10.1086/172149
121. A. Lawrence, M. Elvis, Misaligned disks as obscurers in active galaxies. ApJ **714**(1), 561–570 (2010). https://doi.org/10.1088/0004-637X/714/1/561
122. C. Leipski, H. Falcke, N. Bennert et al., The radio structure of radio-quiet quasars. A&A **455**(1), 161–172 (2006). https://doi.org/10.1051/0004-6361:20054311. arXiv:astro-ph/0606540 [astro-ph]
123. A. Li, Dust in Active Galactic Nuclei. In: Ho LC, Wang JW (eds) The Central Engine of Active Galactic Nuclei, p 561 (2007)
124. N. López-Gonzaga, L. Burtscher, K.R.W. Tristram et al., Mid-infrared interferometry of 23 AGN tori: on the significance of polar-elongated emission. A&A **591**, A47 (2016). https://doi.org/10.1051/0004-6361/201527590. arXiv:1602.05592 [astro-ph.GA]
125. Z. Loska, B. Czerny, R. Szczerba, Irradiation of accretion discs in active galactic nuclei due to the presence of a warm absorber. Mon. Not. R. Astron. Soc. **355**(4), 1080–1090 (2004). https://doi.org/10.1111/j.1365-2966.2004.08387.x. arXiv:astro-ph/0409221 [astro-ph]
126. A.G. Markowitz, M. Krumpe, R. Nikutta, First X-ray-based statistical tests for clumpy-torus models: eclipse events from 230 years of monitoring of Seyfert AGN. MNRAS **439**(2), 1403–1458 (2014). https://doi.

org/10.1093/mnras/stt2492. arXiv:1402.2779 [astro-ph.GA]
127. M.L. Martínez-Aldama, M. Zajaček, B. Czerny et al., Scatter analysis along the multidimensional radius-luminosity relations for reverberation-mapped Mg II sources. ApJ **903**(2), 86 (2020). https://doi.org/10.3847/1538-4357/abb6f8. arXiv:2007.09955 [astro-ph.GA]
128. G. Matt, M. Guainazzi, R. Maiolino, Changing look: from Compton-thick to Compton-thin, or the rebirth of fossil active galactic nuclei. MNRAS **342**(2), 422–426 (2003). https://doi.org/10.1046/j.1365-8711.2003.06539.x. arXiv:astro-ph/0302328 [astro-ph]
129. D.L. Meier, Black Hole Astrophysics: The Engine Paradigm (Springer. Berlin (2012). https://doi.org/10.1007/978-3-642-01936-4
130. F. Melia, H. Falcke, The supermassive black hole at the Galactic center. ARA&A **39**, 309–352 (2001). https://doi.org/10.1146/annurev.astro.39.1.309. arXiv:astro-ph/0106162 [astro-ph]
131. P.G. Mezger, R. Zylka, C.J. Salter et al., Continuum observations of SGR A at mm/submm wavelengths. A&A **209**, 337–348 (1989)
132. P.G. Mezger, W.J. Duschl, R. Zylka, The galactic center: A laboratory for AGN? A&Ar **7**(4), 289–388 (1996). https://doi.org/10.1007/s001590050007
133. J.S. Miller, R.W. Goodrich, W.G. Mathews, Multidirectional views of the active nucleus of NGC 1068. ApJ **378**, 47 (1991). https://doi.org/10.1086/170406
134. T. Minezaki, Y. Yoshii, Y. Kobayashi et al., Reverberation measurements of the inner radii of the dust tori in Quasars. ApJ **886**(2), 150 (2019). https://doi.org/10.3847/1538-4357/ab4f7b. arXiv:1910.08722 [astro-ph.GA]
135. E. Moravec, J. Svoboda, A. Borkar et al., Do radio active galactic nuclei reflect X-ray binary spectral states? A&A **662**, A28 (2022). https://doi.org/10.1051/0004-6361/202142870. arXiv:2202.11116 [astro-ph.GA]
136. L. Moser, Á. Sánchez-Monge, A. Eckart et al., Approaching hell's kitchen: molecular daredevil clouds in the vicinity of sagittarius A*. A&A **603**, A68 (2017). https://doi.org/10.1051/0004-6361/201628385. arXiv:1603.00801 [astro-ph.GA]
137. A.L. Müller, M.H. Naddaf, M. Zajaček et al., Non-thermal emission from fall-back clouds in the broad-line region of active Galactic nuclei. ApJ **931**(1), 39 (2022). https://doi.org/10.3847/1538-4357/ac660a. arXiv:2204.05361 [astro-ph.HE]
138. F. Müller-Sánchez, M.A. Prieto, E.K.S. Hicks et al., Outflows from Active Galactic nuclei: kinematics of the narrow-line and coronal-line regions in seyfert galaxies. ApJ **739**(2), 69 (2011). https://doi.org/10.1088/0004-637X/739/2/69. arXiv:1107.3140 [astro-ph.CO]
139. N. Murray, J. Chiang, S.A. Grossman et al., Accretion disk winds from active Galactic nuclei. Astrophys J **451**, 498 (1995). https://doi.org/10.1086/176238
140. M.H. Naddaf, B. Czerny, Radiation pressure on dust explaining the low ionized broad emission lines in active galactic nuclei. Dust as an important driver of line shape. Astron. Astrophys. **663**, A77 (2022). https://doi.org/10.1051/0004-6361/202142806. arXiv:2111.14963 [astro-ph.GA]
141. M.H. Naddaf, B. Czerny, R. Szczerba, BLR size in realistic FRADO model: the role of shielding effect. Front. Astron. Space Sci. **7**, 15 (2020). https://doi.org/10.3389/fspas.2020.00015. arXiv:2004.01988 [astro-ph.GA]
142. M.H. Naddaf, B. Czerny, R. Szczerba, The picture of BLR in 2.5D FRADO: dynamics and geometry. Astrophys. J. **920**(1), 30 (2021). https://doi.org/10.3847/1538-4357/ac139d. arXiv:2102.00336 [astro-ph.GA]
143. K. Nandra, K.A. Pounds, GINGA observations of the X-ray spectra of Seyfert galaxies. MNRAS **268**, 405–429 (1994). https://doi.org/10.1093/mnras/268.2.405
144. R. Narayan, I. Yi, Advection-dominated accretion: a self-similar solution. ApJ **428**, L13 (1994). https://doi.org/10.1086/187381. arXiv:astro-ph/9403052 [astro-ph]
145. R. Narayan, R. Mahadevan, J.E. Grindlay et al., Advection-dominated accretion model of Sagittarius A*: evidence for a black hole at the Galactic center. ApJ **492**(2), 554–568 (1998). https://doi.org/10.1086/305070. arXiv:astro-ph/9706112 [astro-ph]
146. R. Narayan, I.V. Igumenshchev, M.A. Abramowicz, Magnetically arrested disk: an energetically efficient accretion flow. PASJ **55**, L69–L72 (2003). https://doi.org/10.1093/pasj/55.6.L69. arXiv:astro-ph/0305029 [astro-ph]
147. R. Narayan, A. Chael, K. Chatterjee et al., Jets in magnetically arrested hot accretion flows: geometry, power, and black hole spin-down. MNRAS **511**(3), 3795–3813 (2022). https://doi.org/10.1093/mnras/stac285. arXiv:2108.12380 [astro-ph.HE]
148. C.A. Negrete, D. Dultzin, P. Marziani et al., Highly accreting quasars: the SDSS low-redshift catalog. A&A **620**, A118 (2018). https://doi.org/10.1051/0004-6361/201833285. arXiv:1809.08310 [astro-ph.GA]
149. M. Nenkova, M.M. Sirocky, Ž Ivezić et al., AGN dusty tori. I. Handling of clumpy media. ApJ **685**(1), 147–159 (2008). https://doi.org/10.1086/590482. arXiv:0806.0511 [astro-ph]
150. M. Nenkova, M.M. Sirocky, R. Nikutta et al., AGN dusty tori. II. Observational implications of clumpiness. ApJ **685**(1), 160–180 (2008). https://doi.org/10.1086/590483. arXiv:0806.0512 [astro-ph]
151. H. Netzer, Revisiting the unified model of active Galactic nuclei. Ann. Rev. Astron. Astrophys. **53**, 365–408 (2015). https://doi.org/10.1146/annurev-astro-082214-122302. arXiv:1505.00811 [astro-ph.GA]
152. H. Netzer, A. Laor, Dust in the narrow-line region of active Galactic nuclei. ApJ **404**, L51 (1993). https://doi.org/10.1086/186741
153. H. Netzer, C. Lani, R. Nordon et al., Star formation black hole growth and dusty tori in the most luminous AGNs at z=2-3.5. ApJ **819**(2), 123 (2016). https://doi.org/10.3847/0004-637X/819/2/123. arXiv:1511.07876 [astro-ph.GA]
154. G. Neugebauer, J.B. Oke, E.E. Becklin et al., Absolute spectral energy distribution of quasi-stellar objects from 0.3 to 10 microns. ApJ **230**, 79–94 (1979). https://doi.org/10.1086/157063
155. F. Nicastro, A. Martocchia, G. Matt, The lack of broad-line regions in low accretion rate active galactic nuclei as evidence of their origin in the accretion

disk. ApJ **589**(1), L13–L16 (2003). https://doi.org/10.1086/375715. arXiv:astro-ph/0304128 [astro-ph]
156. S. Nishiyama, T. Nagata, M. Tamura et al., The interstellar extinction law toward the Galactic center. II. V, J, H, and K_s bands. ApJ **680**(2), 1174–1179 (2008). https://doi.org/10.1086/587791. arXiv:0802.3559 [astro-ph]
157. F. Nogueras-Lara, R. Schödel, N. Neumayer et al., GALACTICNUCLEUS: a high angular-resolution JHK_s imaging survey of the Galactic centre. III. Evidence for wavelength-dependence of the extinction curve in the near-infrared. A&A **641**, A141 (2020). https://doi.org/10.1051/0004-6361/202038606. arXiv:2007.04401 [astro-ph.GA]
158. I.D. Novikov, K.S. Thorne, Astrophysics of black holes. In: Black Holes (Les Astres Occlus), pp 343–450 (1973)
159. V.L. Oknyanskij, On the possibility for measuring the hubble constant from optical-to-NIR variability time delay in AGNs. Odessa Astron. Publ. **12**, 99 (1999). arXiv:2208.09295 [astro-ph.GA]
160. V.L. Oknyanskij, V.M. Lyuty, O.G. Taranova et al., On the correlation of IR and optical variability in NGC 4151. Odessa Astron. Publ. **21**, 79 (2008)
161. D.E. Osterbrock, Ionized gas and dust in active galactic nuclei. AJ **84**, 901–909 (1979). https://doi.org/10.1086/112494
162. D.E. Osterbrock, G.J. Ferland, *Astrophysics of gaseous nebulae and active galactic nuclei* (University Science Books, Sausalito, CA, 2006)
163. D.E. Osterbrock, R.W. Pogge, The spectra of narrow-line Seyfert 1 galaxies. ApJ **297**, 166–176 (1985). https://doi.org/10.1086/163513
164. T. Ott, A. Eckart, R. Genzel, Variable and embedded stars in the Galactic center. ApJ **523**(1), 248–264 (1999). https://doi.org/10.1086/307712
165. P. Padovani, D.M. Alexander, R.J. Assef et al., Active galactic nuclei: What's in a name? A&Ar **25**(1), 2 (2017). https://doi.org/10.1007/s00159-017-0102-9. arXiv:1707.07134 [astro-ph.GA]
166. X. Pan, S.L. Li, X. Cao et al., A disk instability model for the quasi-periodic eruptions of GSN 069. ApJ **928**(2), L18 (2022). https://doi.org/10.3847/2041-8213/ac5faf. arXiv:2203.12137 [astro-ph.GA]
167. S. Panda, The CaFe project: optical Fe II and near-infrared Ca II triplet emission in active galaxies: simulated EWs and the co-dependence of cloud size and metal content. A&A **650**, A154 (2021). https://doi.org/10.1051/0004-6361/202140393. arXiv:2004.13113 [astro-ph.GA]
168. S. Panda, P. Marziani, High Eddington accreting quasar spectra as discovery tools: current state and challenges (2022). arXiv e-prints arXiv:2210.15041
169. S. Panda, E.J. Skorek, Metallicity evolution in quasars (2021). arXiv e-prints arXiv:2111.14516 [astro-ph.GA]
170. S. Panda, M. Śniegowska, Changing-Look AGNs – I. Tracking the transition on the main sequence of quasars (2022). arXiv e-prints arXiv:2206.10056 [astro-ph.HE]
171. S. Panda, B. Czerny, T.P. Adhikari et al., Modeling of the quasar main sequence in the optical plane. ApJ **866**(2), 115 (2018). https://doi.org/10.3847/1538-4357/aae209. arXiv:1806.08571 [astro-ph.HE]
172. S. Panda, P. Marziani, B. Czerny, The quasar main sequence explained by the combination of eddington ratio, metallicity, and orientation. ApJ **882**(2), 79 (2019). https://doi.org/10.3847/1538-4357/ab3292. arXiv:1905.01729 [astro-ph.HE]
173. F. Peißker, S.E. Hosseini, M. Zajaček et al., Monitoring dusty sources in the vicinity of Sagittarius A*. A&A **634**, A35 (2020). https://doi.org/10.1051/0004-6361/201935953. arXiv:1911.00321 [astro-ph.GA]
174. F. Peißker, M. Zajaček, A. Eckart et al., The apparent tail of the Galactic center object G2/DSO. ApJ **923**(1), 69 (2021). https://doi.org/10.3847/1538-4357/ac23df. arXiv:2112.04543 [astro-ph.GA]
175. B.M. Peterson, A. Wandel, Keplerian motion of broad-line region gas as evidence for supermassive black holes in active Galactic nuclei. Astrophys. J. Lett. **521**(2), L95–L98 (1999). https://doi.org/10.1086/312190. arXiv:astro-ph/9905382 [astro-ph]
176. B.M. Peterson, L. Ferrarese, K.M. Gilbert et al., Central masses and broad-line region sizes of active Galactic nuclei. II. A homogeneous analysis of a large reverberation-mapping database. ApJ **613**(2), 682–699 (2004). https://doi.org/10.1086/423269. arXiv:astro-ph/0407299 [astro-ph]
177. P.O. Petrucci, J. Ferreira, G. Henri et al., The role of the disc magnetization on the hysteresis behaviour of X-ray binaries. MNRAS **385**(1), L88–L92 (2008). https://doi.org/10.1111/j.1745-3933.2008.00439.x. arXiv:0712.3388 [astro-ph]
178. E.A. Pier, J.H. Krolik, Infrared spectra of obscuring dust tori around active Galactic nuclei. I. Calculational method and basic trends. ApJ **401**, 99 (1992). https://doi.org/10.1086/172042
179. J.M. Pittard, J.E. Dyson, S.A.E.G. Falle et al., The formation of broad emission line regions in supernova-QSO wind interactions. A&A **375**, 827–839 (2001). https://doi.org/10.1051/0004-6361:20010906. arXiv:astro-ph/0107101 [astro-ph]
180. P. Predehl, R.A. Sunyaev, W. Becker et al., Detection of large-scale X-ray bubbles in the Milky Way halo. Nature **588**(7837), 227–231 (2020). https://doi.org/10.1038/s41586-020-2979-0. arXiv:2012.05840 [astro-ph.GA]
181. R. Prince, K. Hryniewicz, S. Panda et al., Viewing angle observations and effects of evolution with Redshift, Black Hole Mass, and Eddington Ratio in quasar-based cosmology. ApJ **925**(2), 215 (2022). https://doi.org/10.3847/1538-4357/ac3f36. arXiv:2106.03877 [astro-ph.GA]
182. D. Proga, J.M. Stone, T.R. Kallman, Dynamics of line-driven disk winds in active Galactic nuclei. Astrophys. J. **543**(2), 686–696 (2000). https://doi.org/10.1086/317154. arXiv:astro-ph/0005315 [astro-ph]
183. S. Rakshit, C.S. Stalin, J. Kotilainen, Spectral properties of quasars from sloan digital sky survey data release 14: the catalog. ApJs **249**(1), 17 (2020). https://doi.org/10.3847/1538-4365/ab99c5. arXiv:1910.10395 [astro-ph.GA]
184. C. Ramos Almeida, C. Ricci, Nuclear obscuration in active galactic nuclei. Nat. Astron. **1**, 679–689 (2017). https://doi.org/10.1038/s41550-017-0232-z. arXiv:1709.00019 [astro-ph.GA]
185. C. Ramos Almeida, M.J. Martínez González, A. Asensio Ramos et al., Upholding the unified model for active galactic nuclei: VLT/FORS2 spectropolarime-

try of Seyfert 2 galaxies. MNRAS **461**(2), 1387–1403 (2016). https://doi.org/10.1093/mnras/stw1388. arXiv:1606.02204 [astro-ph.GA]
186. C. Rauch, K. Mužić, A. Eckart et al., A peek behind the dusty curtain: K_S-band polarization photometry and bow shock models of the Galactic center source IRS 8. A&A **551**, A35 (2013). https://doi.org/10.1051/0004-6361/201219874
187. P.F. Roche, C. Packham, D.K. Aitken et al., Silicate absorption in heavily obscured galaxy nuclei. MNRAS **375**(1), 99–104 (2007). https://doi.org/10.1111/j.1365-2966.2006.11207.x. arXiv:astro-ph/0610583 [astro-ph]
188. P.F. Roche, E. Lopez-Rodriguez, C.M. Telesco et al., The magnetic field in the central parsec of the Galaxy. MNRAS **476**(1), 235–245 (2018). https://doi.org/10.1093/mnras/sty129. arXiv:1802.06634 [astro-ph.GA]
189. A. Różańska, Thermal conduction between an accretion disc and a corona in active galactic nuclei: vertical structure of the transition layer. MNRAS **308**(3), 751–762 (1999). https://doi.org/10.1046/j.1365-8711.1999.02752.x
190. A. Różańska, B. Czerny, D. Kunneriath et al., Conditions for thermal instability in the Galactic Centre mini-spiral region. MNRAS **445**(4), 4385–4394 (2014). https://doi.org/10.1093/mnras/stu2066. arXiv:1410.0397 [astro-ph.HE]
191. A. Różańska, D. Kunneriath, B. Czerny et al., Multiphase environment of compact galactic nuclei: the role of the nuclear star cluster. MNRAS **464**(2), 2090–2102 (2017). https://doi.org/10.1093/mnras/stw2460. arXiv:1609.08834 [astro-ph.GA]
192. J. Sanchez-Bermudez, R. Schödel, A. Alberdi et al., Properties of bow-shock sources at the Galactic center. A&A **567**, A21 (2014). https://doi.org/10.1051/0004-6361/201423657. arXiv:1405.4528 [astro-ph.SR]
193. E.O. Schmidt, G.A. Oio, D. Ferreiro et al., Asymmetric emission of the [OIII]λ5007 profile in narrow-line Seyfert 1 galaxies. A&A **615**, A13 (2018). https://doi.org/10.1051/0004-6361/201731557. arXiv:1802.00072 [astro-ph.GA]
194. R. Schödel, F. Najarro, K. Muzic et al., Peering through the veil: near-infrared photometry and extinction for the Galactic nuclear star cluster. Accurate near infrared H, Ks, and L' photometry and the near-infrared extinction-law toward the central parsec of the Galaxy. A&A **511**, A18 (2010). https://doi.org/10.1051/0004-6361/200913183
195. R.O. Sexton, W. Matzko, N. Darden et al., Bayesian AGN Decomposition Analysis for SDSS spectra: a correlation analysis of [O III] λ5007 outflow kinematics with AGN and host galaxy properties. MNRAS **500**(3), 2871–2895 (2021). https://doi.org/10.1093/mnras/staa3278. arXiv:2010.09748 [astro-ph.GA]
196. C.K. Seyfert, Nuclear emission in spiral nebulae. ApJ **97**, 28 (1943). https://doi.org/10.1086/144488
197. E.S. Shablovinskaya, V.L. Afanasiev, Popović Lč, Measuring the AGN sublimation radius with a new approach: reverberation mapping of broad line polarization. ApJ **892**(2), 118 (2020). https://doi.org/10.3847/1538-4357/ab7849. arXiv:2003.12809 [astro-ph.GA]
198. E.S. Shablovinskaya, V.L. Afanasiev, Popović Lč, Measuring the AGN sublimation radius with a new approach: reverberation mapping of broad line polarization. ApJ **892**(2), 118 (2020). https://doi.org/10.3847/1538-4357/ab7849. arXiv:2003.12809 [astro-ph.GA]
199. N.I. Shakura, R.A. Sunyaev, Black holes in binary systems. Observational appearance. Astron. Astrophys. **24**, 337–355 (1973)
200. Y. Shen, G.T. Richards, M.A. Strauss et al., A catalog of quasar properties from sloan digital sky survey data release 7. ApJs **194**(2), 45 (2011). https://doi.org/10.1088/0067-0049/194/2/45. arXiv:1006.5178 [astro-ph.CO]
201. I. Shlosman, M.C. Begelman, Evolution of self-gravitating accretion disks in active Galactic nuclei. ApJ **341**, 685 (1989). https://doi.org/10.1086/167526
202. R. Siebenmorgen, M. Haas, E. Krügel et al., Discovery of 10 μm silicate emission in quasars. Evidence of the AGN unification scheme. A&A **436**(1), L5–L8 (2005). https://doi.org/10.1051/0004-6361:200500109
203. R. Siebenmorgen, F. Heymann, A. Efstathiou, Self-consistent two-phase AGN torus models$\star$. SED library for observers. A&A **583**, A120 (2015). https://doi.org/10.1051/0004-6361/201526034. arXiv:1508.04343 [astro-ph.GA]
204. M. Sniegowska, B. Czerny, E. Bon et al., Possible mechanism for multiple changing-look phenomena in active galactic nuclei. Astron. Astrophys. **641**, A167 (2020). https://doi.org/10.1051/0004-6361/202038575. arXiv:2007.06441 [astro-ph.GA]
205. M. Śniegowska, P. Marziani, B. Czerny et al., High metal content of highly accreting quasars. ApJ **910**(2), 115 (2021). https://doi.org/10.3847/1538-4357/abe1c8. arXiv:2009.14177 [astro-ph.HE]
206. M. Śniegowska, M. Grzędzielski, B. Czerny, et al Modified models of radiation pressure instability in application to 10, 10^5, and 10^7 $M_\odot$ accreting black holes (2022). arXiv e-prints arXiv:2204.10067 [astro-ph.HE]
207. M.A. Sobolewska, A. Siemiginowska, M. Gierliński, Simulated spectral states of active galactic nuclei and observational predictions. MNRAS **413**(3), 2259–2268 (2011). https://doi.org/10.1111/j.1365-2966.2011.18302.x. arXiv:1102.0798 [astro-ph.GA]
208. C. Sobrino Figaredo, M. Haas, M. Ramolla, et al Dust Reverberation of 3C 273: Torus Structure and Lag-Luminosity Relation. AJ **159**(6), 259 (2020). https://doi.org/10.3847/1538-3881/ab89b1, arXiv:2004.10244 [astro-ph.GA]
209. S. Solanki, S.M. Ressler, L. Murchikova, et al The Inner 2 pc of Sagittarius A*: Simulations of the Circumnuclear Disk and Multiphase Gas Accretion in the Galactic Center (2023). arXiv e-prints . https://doi.org/10.48550/arXiv.2301.07735, arXiv:2301.07735 [astro-ph.HE]
210. M. Stalevski, J. Fritz, M. Baes et al., 3D radiative transfer modelling of the dusty tori around active galactic nuclei as a clumpy two-phase medium. MNRAS **420**(4), 2756–2772 (2012). https://doi.org/10.1111/j.1365-2966.2011.19775.x. arXiv:1109.1286 [astro-ph.CO]
211. M. Stalevski, C. Ricci, Y. Ueda et al., The dust covering factor in active galactic nuclei. MNRAS **458**(3), 2288–

2302 (2016). https://doi.org/10.1093/mnras/stw444. arXiv:1602.06954 [astro-ph.GA]
212. M. Stalevski, D. Asmus, K.R.W. Tristram, Dissecting the active galactic nucleus in Circinus - I. Peculiar mid-IR morphology explained by a dusty hollow cone. MNRAS **472**(4), 3854–3870 (2017). https://doi.org/10.1093/mnras/stx2227. arXiv:1708.07838 [astro-ph.GA]
213. M. Stalevski, K.R.W. Tristram, D. Asmus, Dissecting the active galactic nucleus in Circinus - II. A thin dusty disc and a polar outflow on parsec scales. MNRAS **484**(3), 3334–3355 (2019). https://doi.org/10.1093/mnras/stz220. arXiv:1901.05488 [astro-ph.GA]
214. J. Stern, A. Laor, A. Baskin, Radiation pressure confinement - I. Ionized gas in the ISM of AGN hosts. MNRAS **438**(2), 901–921 (2014). https://doi.org/10.1093/mnras/stt1843. arXiv:1309.7825 [astro-ph.CO]
215. T. Storchi-Bergmann, Observational Overview of the Feeding of Active Galactic Nuclei. In: Revista Mexicana de Astronomia y Astrofisica Conference Series, pp 139–146 (2008), https://doi.org/10.48550/arXiv.0712.3747, arXiv:0712.3747
216. M. Su, T.R. Slatyer, D.P. Finkbeiner, Giant Gamma-ray bubbles from Fermi-LAT: Active Galactic nucleus activity or bipolar galactic wind? ApJ **724**(2), 1044–1082 (2010). https://doi.org/10.1088/0004-637X/724/2/1044. arXiv:1005.5480 [astro-ph.HE]
217. J.W. Sulentic, P. Marziani, D. Dultzin-Hacyan, Phenomenology of broad emission lines in active Galactic nuclei. ARA&A **38**, 521–571 (2000). https://doi.org/10.1146/annurev.astro.38.1.521
218. R. Sunyaev, E. Churazov, Equivalent width, shape and proper motion of the iron fluorescent line emission from molecular clouds as an indicator of the illuminating source X-ray flux history. MNRAS **297**(4), 1279–1291 (1998). https://doi.org/10.1046/j.1365-8711.1998.01684.x. arXiv:astro-ph/9805038 [astro-ph]
219. R.A. Sunyaev, M. Markevitch, M. Pavlinsky, The center of the galaxy in the recent past: a view from GRANAT. ApJ **407**, 606 (1993). https://doi.org/10.1086/172542
220. A. Tanner, A.M. Ghez, M. Morris et al., Spatially resolved observations of the Galactic center source IRS 21. ApJ **575**(2), 860–870 (2002). https://doi.org/10.1086/341470. arXiv:astro-ph/0204372 [astro-ph]
221. A.M. Tanner, A.M. Ghez, M. Morris et al., Resolving the Northern arm sources at the Galactic center. Astronomische Nachrichten Suppl. **324**(1), 597–603 (2003). https://doi.org/10.1002/asna.200385093
222. R. Tazaki, K. Ichikawa, M. Kokubo, Dust destruction by charging: a possible origin of gray extinction curves of active Galactic nuclei. ApJ **892**(2), 84 (2020). https://doi.org/10.3847/1538-4357/ab7822. arXiv:2002.08023 [astro-ph.GA]
223. F. Tombesi, M. Cappi, J.N. Reeves et al., Evidence for ultra-fast outflows in radio-quiet AGNs. I. Detection and statistical incidence of Fe K-shell absorption lines. A&A **521**, A57 (2010). https://doi.org/10.1051/0004-6361/200913440. arXiv:1006.2858 [astro-ph.HE]
224. A.A. Trani, M. Mapelli, A. Ballone, Forming circumnuclear disks and rings in galactic nuclei: a competition between supermassive Black Hole and nuclear star cluster. ApJ **864**(1), 17 (2018). https://doi.org/10.3847/1538-4357/aad414. arXiv:1807.09780 [astro-ph.GA]
225. A. Trinca, R. Schneider, R. Maiolino et al., Seeking the growth of the first black hole seeds with JWST. MNRAS **519**(3), 4753–4764 (2023). https://doi.org/10.1093/mnras/stac3768. arXiv:2211.01389 [astro-ph.GA]
226. A. Trova, V. Karas, P. Slaný et al., Electrically charged matter in permanent rotation around magnetized black holes: a toy model for self-gravitating fluid tori. ApJs **226**(1), 12 (2016). https://doi.org/10.3847/0067-0049/226/1/12. arXiv:1608.03427 [astro-ph.HE]
227. A. Trova, E. Hackmann, V. Karas et al., Influence of test charge and uniform magnetic field on charged fluid equilibrium structures. Phys. Rev. **101**(8), 083027 (2020). https://doi.org/10.1103/PhysRevD.101.083027
228. M. Tsuboi, Y. Kitamura, K. Uehara et al., ALMA view of the Galactic center minispiral: ionized gas flows around sagittarius A*. ApJ **842**(2), 94 (2017). https://doi.org/10.3847/1538-4357/aa74e3. arXiv:1608.08714 [astro-ph.GA]
229. T. Tsuchikawa, H. Kaneda, S. Oyabu et al., A systematic study of silicate absorption features in heavily obscured AGNs observed by Spitzer/IRS. A&A **651**, A117 (2021). https://doi.org/10.1051/0004-6361/202140483. arXiv:2105.04792 [astro-ph.GA]
230. U V, Lai T, Bianchin M, et al., GOALS-JWST: Resolving the Circumnuclear Gas Dynamics in NGC 7469 in the Mid-infrared. ApJ **940**(1), L5 (2022). https://doi.org/10.3847/2041-8213/ac961c. arXiv:2209.01210 [astro-ph.GA]
231. C.M. Urry, P. Padovani, Unified schemes for radio-loud active Galactic nuclei. PASP **107**, 803 (1995). https://doi.org/10.1086/133630. arXiv:astro-ph/9506063 [astro-ph]
232. M.P. Véron-Cetty, P. Véron, A catalogue of quasars and active nuclei: 13th edition. A&A **518**, A10 (2010). https://doi.org/10.1051/0004-6361/201014188
233. S.V. Vladimirov, K. Ostrikov, A.A. Samarian, Physics and applications of complex plasmas (2005)
234. B. Vollmer, W.J. Duschl, The minispiral in the Galactic center revisited. New **4**(8), 581–590 (2000). https://doi.org/10.1016/S1384-1076(99)00043-3. arXiv:astro-ph/9904096 [astro-ph]
235. K. Wada, M. Schartmann, R. Meijerink, Multiphase nature of a radiation-driven fountain with nuclear starburst in a low-mass active Galactic nucleus. ApJ **828**(2), L19 (2016). https://doi.org/10.3847/2041-8205/828/2/L19. arXiv:1608.06995 [astro-ph.GA]
236. E.J. Wampler, N.N. Chugai, P. Petitjean, The absorption spectrum of nuclear gas in Q0059–2735. ApJ **443**, 586 (1995). https://doi.org/10.1086/175551
237. A. Wandel, B.M. Peterson, M.A. Malkan, Central masses and broad-line region sizes of active Galactic nuclei. I. Comparing the photoionization and reverberation techniques. Astrophys. J. **526**(2), 579–591 (1999). https://doi.org/10.1086/308017. arXiv:astro-ph/9905224 [astro-ph]
238. H. Wang, F. Xing, K. Zhang et al., Outflow and hot dust emission in high-redshift quasars. ApJ **776**(1),

L15 (2013). https://doi.org/10.1088/2041-8205/776/1/L15. arXiv:1309.4465 [astro-ph.CO]
239. Q.D. Wang, M.A. Nowak, S.B. Markoff et al., Dissecting X-ray-emitting gas around the center of our galaxy. Science **341**(6149), 981–983 (2013). https://doi.org/10.1126/science.1240755. arXiv:1307.5845 [astro-ph.HE]
240. T. Waters, D. Proga, R. Dannen, Multiphase AGN winds from X-Ray-irradiated disk atmospheres. ApJ **914**(1), 62 (2021). https://doi.org/10.3847/1538-4357/abfbe6. arXiv:2101.09273 [astro-ph.GA]
241. T. Waters, D. Proga, R. Dannen et al., Dynamical thermal instability in highly supersonic outflows. ApJ **931**(2), 134 (2022). https://doi.org/10.3847/1538-4357/ac6612. arXiv:2111.07440 [astro-ph.GA]
242. J.C. Weingartner, B.T. Draine, Dust grain-size distributions and extinction in the Milky Way, Large Magellanic Cloud, and Small Magellanic Cloud. ApJ **548**(1), 296–309 (2001). https://doi.org/10.1086/318651. arXiv:astro-ph/0008146 [astro-ph]
243. J.C. Weingartner, B.T. Draine, D.K. Barr, Photoelectric emission from dust grains exposed to extreme ultraviolet and X-ray radiation. ApJ **645**(2), 1188–1197 (2006). https://doi.org/10.1086/504420. arXiv:astro-ph/0601296 [astro-ph]
244. R.J. Weymann, S.L. Morris, C.B. Foltz et al., Comparisons of the emission-line and continuum properties of broad absorption line and normal quasi-stellar objects. ApJ **373**, 23 (1991). https://doi.org/10.1086/170020
245. M. Wielgus, M. Moscibrodzka, J. Vos et al., Orbital motion near Sagittarius A*. Constraints from polarimetric ALMA observations. A&A **665**, L6 (2022). https://doi.org/10.1051/0004-6361/202244493. arXiv:2209.09926 [astro-ph.HE]
246. D. Williamson, S. Hönig, M. Venanzi, Radiation hydrodynamics models of active Galactic nuclei: beyond the central parsec. ApJ **897**(1), 26 (2020). https://doi.org/10.3847/1538-4357/ab989e. arXiv:2006.00918 [astro-ph.GA]
247. B.J. Wills, H. Netzer, D. Wills, Broad emission features in QSOs and active galactic nuclei. II. New observations and theory of Fe II and HI emission. ApJ **288**, 94–116 (1985). https://doi.org/10.1086/162767
248. G. Witzel, B.N. Sitarski, A.M. Ghez et al., The post-periapsis evolution of Galactic center source G1: the second case of a resolved tidal interaction with a supermassive black hole. ApJ **847**(1), 80 (2017). https://doi.org/10.3847/1538-4357/aa80ea. arXiv:1707.02301 [astro-ph.GA]
249. G. Witzel, G. Martinez, S.P. Willner et al., Rapid variability of Sgr A* across the electromagnetic spectrum. ApJ **917**(2), 73 (2021). https://doi.org/10.3847/1538-4357/ac0891. arXiv:2011.09582 [astro-ph.HE]
250. D. Wylezalek, A. Vayner, D.S.N. Rupke et al., First results from the JWST early release science program Q3D: turbulent times in the life of a z 3 extremely red quasar revealed by NIRSpec IFU. ApJ **940**(1), L7 (2022). https://doi.org/10.3847/2041-8213/ac98c3. arXiv:2210.10074 [astro-ph.GA]
251. Y. Xie, L.C. Ho, The ionization and destruction of polycyclic aromatic hydrocarbons in powerful quasars. ApJ **925**(2), 218 (2022). https://doi.org/10.3847/1538-4357/ac32e2. arXiv:2110.09705 [astro-ph.GA]
252. Q. Yang, X.B. Wu, X. Fan et al., Discovery of 21 new changing-look AGNs in the Northern sky. ApJ **862**(2), 109 (2018). https://doi.org/10.3847/1538-4357/aaca3a. arXiv:1711.08122 [astro-ph.GA]
253. F. Yuan, R. Narayan, Hot accretion flows around black holes. ARA&A **52**, 529–588 (2014). https://doi.org/10.1146/annurev-astro-082812-141003. arXiv:1401.0586 [astro-ph.HE]
254. M. Zajaček, V. Karas, A. Eckart, Dust-enshrouded star near supermassive black hole: predictions for high-eccentricity passages near low-luminosity galactic nuclei. A&A **565**, A17 (2014). https://doi.org/10.1051/0004-6361/201322713. arXiv:1403.5792 [astro-ph.GA]
255. M. Zajaček, S. Britzen, A. Eckart et al., Nature of the Galactic centre NIR-excess sources. I. What can we learn from the continuum observations of the DSO/G2 source? A&A **602**, A121 (2017). https://doi.org/10.1051/0004-6361/201730532. arXiv:1704.03699 [astro-ph.GA]
256. M. Zajaček, B. Czerny, M.L. Martinez-Aldama et al., Time-delay measurement of Mg II broad-line response for the highly accreting quasar HE 0413–4031: implications for the Mg II-based radius-luminosity relation. ApJ **896**(2), 146 (2020). https://doi.org/10.3847/1538-4357/ab94ae. arXiv:2005.09071 [astro-ph.GA]
257. M. Zajaček, B. Czerny, M.L. Martinez-Aldama et al., Time delay of Mg II emission response for the luminous quasar HE 0435–4312: toward application of the high-accretor radius-luminosity relation in cosmology. Astrophys. J. **912**(1), 10 (2021). https://doi.org/10.3847/1538-4357/abe9b2. arXiv:2012.12409 [astro-ph.GA]
258. R. Zamanov, P. Marziani, J.W. Sulentic et al., Kinematic linkage between the broad- and narrow-line-emitting gas in active Galactic nuclei. ApJ **576**(1), L9–L13 (2002). https://doi.org/10.1086/342783. arXiv:astro-ph/0207387 [astro-ph]
259. L. Zhang, L.C. Ho, A. Li, Evidence that shocks destroy small PAH molecules in low-luminosity active Galactic nuclei. ApJ **939**(1), 22 (2022). https://doi.org/10.3847/1538-4357/ac930f
260. S. Zhang, J. Ge, T. Ji et al., The 2175 Å bump features in FeLoBAL quasars: one indicator of MW-like dust in the nuclear region of quasars. A&A **663**, A63 (2022). https://doi.org/10.1051/0004-6361/202142476. arXiv:2203.03789 [astro-ph.GA]
261. J.H. Zhao, M.R. Morris, W.M. Goss et al., Dynamics of ionized gas at the Galactic center: very large array observations of the three-dimensional velocity field and location of the ionized streams in Sagittarius A West. ApJ **699**(1), 186–214 (2009). https://doi.org/10.1088/0004-637X/699/1/186. arXiv:0904.3133 [astro-ph.GA]
262. J.H. Zhao, R. Blundell, J.M. Moran et al., The high-density ionized gas in the central parsec of the galaxy. ApJ **723**(2), 1097–1109 (2010). https://doi.org/10.1088/0004-637X/723/2/1097. arXiv:1009.1401 [astro-ph.GA]